



力学专业（硕）博士研究生专业课程

耦合场理论、分析方法 与数值仿真

王省哲

土木工程与力学学院



课程主要内容

- 引言
- 耦合场分析方法简介
 - 间接耦合分析方法
 - 直接耦合分析方法
- 一些耦合场分析专题
 - (包括基本模型、解析和数值分析方法等)
 - 力-热耦合问题
 - 流(气)-固耦合问题
 - (电)磁-力耦合问题
 - 风-沙-电等耦合问题



课程主要目的

- 了解和掌握多场问题的基本特征、耦合的性质与意义；
- 介绍几类典型的多场耦合问题的基本模型与特征；
- 以几类典型的多场耦合问题为例，介绍其分析的方法和思路，从中体会和学习基本的方法；
- 一→用于自己的研究工作或者今后可能遇到的多场耦合问题中



课程学习方式

- 课堂讲授（主）+ 学生个人课后阅读（辅）
- 讲授内容是一些具有典型的文章资料
（包括教师个人的相关专题的研究举例与经历）
- 学生个人阅读主要是提供的资料
+ 个人从事的耦合问题的内容
+ 个人感兴趣的耦合场方向；
- 课程成绩（2部分组成）
总评成绩 = 平时考勤 + （个人汇报） 期末 ← 提交课程报告方式



课程使用资料

- 一些代表性的学术论文（可复印或提供电子版本）
- 参考书目（课后阅读）
 - 1、周又和、郑晓静著，电磁固体结构力学，科学出版社，1999
 - 2、秦庆华、杨庆生著，非均匀材料多场耦合行为的宏细观理论，高等教育出版社，2008
 - 3、赵阳升著，多孔介质多场耦合作用及其工程响应，科学出版社，2010
 - 4、方岱宁著，铁磁固体的变形与断裂，科学出版社，2011
 - 5、Zheng Xiaojing, Mechanics of Wind-blown Sand Movement, Springer-Verlag Press, 2009
- 学生个人结合研究方面和研究兴趣阅读多场方面的文献资料



课程主要内容

1、课程名称与编码： 耦合场理论与数值仿真（026211001）

第一章 耦合场的理论以及一般方法（6学时）

§ 1、耦合场问题的背景、基本特征与一般理论

§ 2、耦合场问题的分类、求解方法

第二章 热弹性耦合问题专题（9学时）

§ 1、热弹性问题的基本特征、方程

§ 2、热弹性耦合问题的解析求解

§ 3、热弹性耦合问题的数值求解以及一些算例

第三章 流—固耦合问题专题（12学时）

§ 1、流—固耦合问题的基本特征、方程

§ 2、流—固性耦合问题的求解及一些算例

§ 3、风—沙三题耦合问题的一些基本特征及算例



课程主要内容

第四章 电磁弹性多场耦合问题专题（18学时）

§ 1、电磁场基本理论简介

§ 2、压电—结构耦合问题的基本理论及方法

§ 3、压电—结构耦合的一些算例

§ 4、磁弹性耦合问题的基本理论及方法

§ 5、磁弹性耦合动力学问题的基本理论及方法

§ 6、载流结构的电—磁—力耦合问题的基本理论及方法

§ 7、一些电—磁—力—热耦合问题的算例

注：另6—9学时安排学生查阅资料、讨论、Project汇报等。



引言

多场耦合问题： (Muti-fields coupling problem)

研究两个或者两个以上的场通过相互作用而形成的物理（或力学）现象的问题。

- ❖ 普遍存在于客观世界
- ❖ 普遍存在于工程应用领域
- ❖ 常见的耦合问题：结构-热耦合、流-固耦合、结构-电、结构-磁耦合等...



❖ 越来越多的耦合问题：与智能材料关联

智能材料(Intelligent material、Smart material、daptive material and structure)是二十世纪90年代迅速发展起来的一类新型复合材料。智能材料就是指具有感知环境（包括内环境和外环境）刺激，对之进行分析、处理、判断，并采取一定的措施进行适度响应的智能特征的材料。

智能材料需具备以下内涵：

- 具有感知功能，能够检测并且可以识别外界(或者内部)的刺激强度，如电、光、热、应力、应变、化学、核辐射等；
- 具有驱动功能，能够响应外界变化；
- 能够按照设定的方式选择和控制响应；
- 反应比较灵敏、及时和恰当；
- 当外部刺激消除后，能够迅速恢复到原始状态。

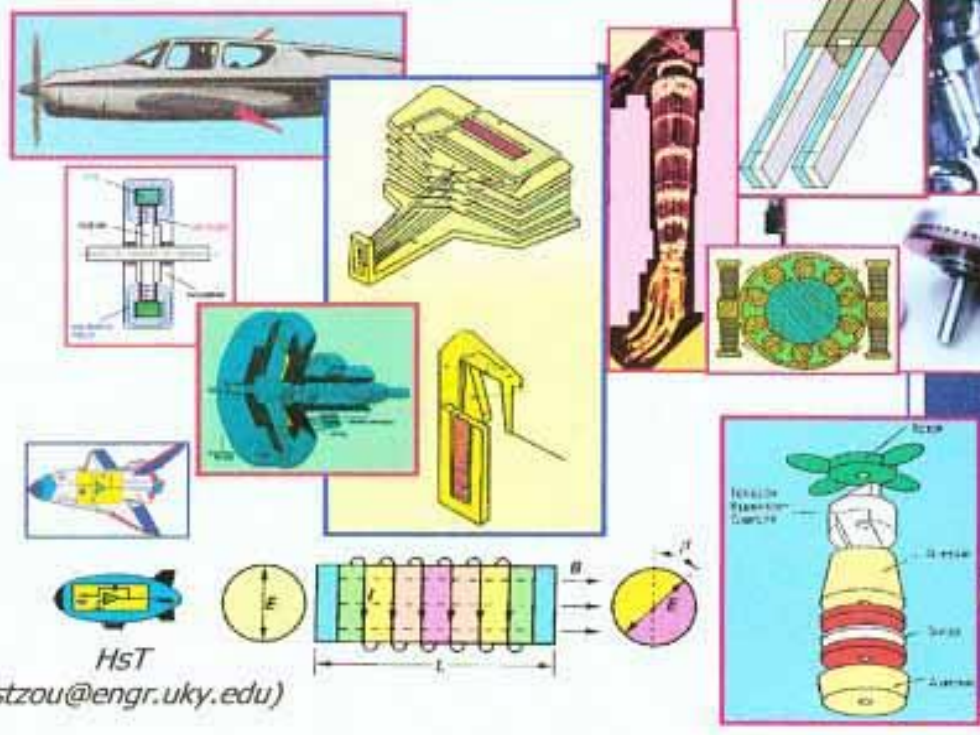


智能材料主要种类

- ✓ 形状记忆合金（复合材料）；
- ✓ 电流变体和磁流变体（液体和弹性体、胶体）；
- ✓ 磁致伸缩材料（复合材料）；
- ✓ 铁电、压电陶瓷、超导、电致伸缩陶瓷；
- ✓ 智能材料系统（电、磁、温度等敏感）；
- ✓ 光、电致变色材料等；
- ✓



**SMART STRUCTURES, PRECISION
STRUCTURONIC AND
MECHATRONIC SYSTEMS WITH
SMART MATERIALS**



HST
(hstzou@engr.uky.edu)

● 多场耦合作用下的材料功能研究是科学技术发展前沿！



耦合的分类:

—— 从耦合的空间属性上分类

Felippa et al. *Comput. meth. Appl. Mech. Engrg.*, 2001

- **区域耦合** —— 整个区域或部分区域内多场共存，各场间无边界。

如：结构-热、结构-电(磁) 耦合...

- **边界耦合** —— 各场间有明显的边界，场之间通过边界作用实现相互作用。

如：流-固耦合、空气-弹性、压电-结构...

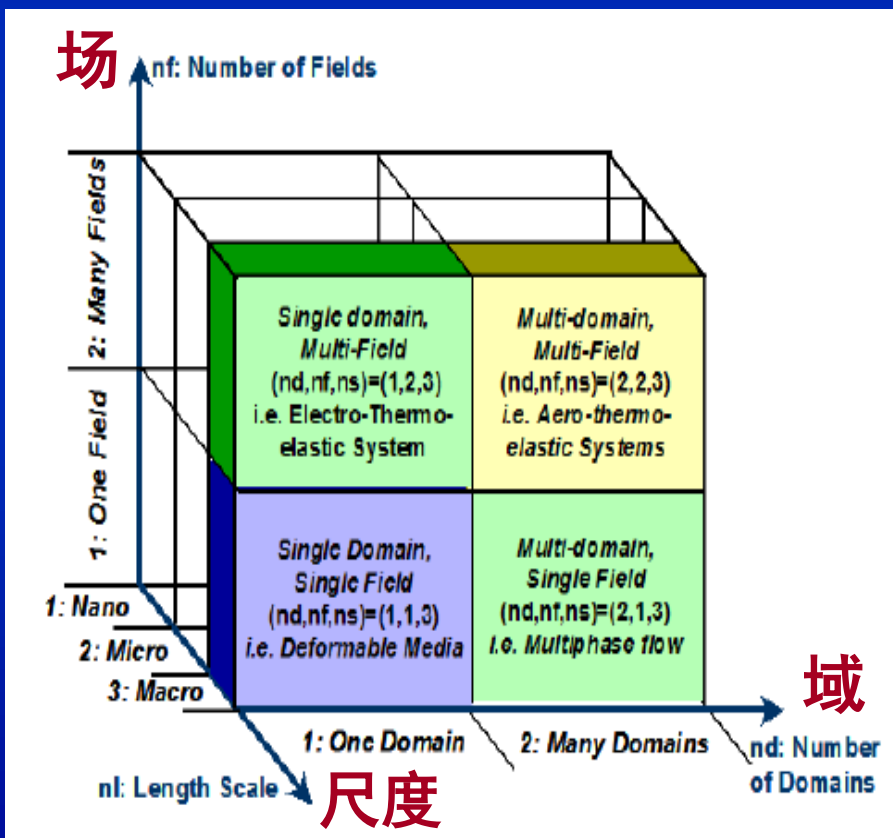


多物理场:
(Multiphysics) { “多场(Multi-field)”
“多区域(Multi-domain)”
“多尺度(Multi-scale)”

系统同时存在多个物理场的激励和响应

“一个”、或“多个”
系统的各个具有不同特征的连续体通过边(交)界之间的相互作用

“纳尺度”、“微尺度”、“宏观尺度”
系统中不同尺度下从微观到宏观行为的连续一致跨越





耦合问题领域几个发展方向（“十一五”学科发展规划）

- ❖ 力-电-磁-热耦合场的分析理论；
- ❖ 智能材料的本构关系；
- ❖ 智能结构动力学与主被动控制；
- ❖ 耦合场的破坏力学、失效机理与智能器件的可靠性；
- ❖ 风-沙耦合、风沙电耦合问题
- ❖ 冻土、岩石，应力场-温度场-流场-空气泡耦合等



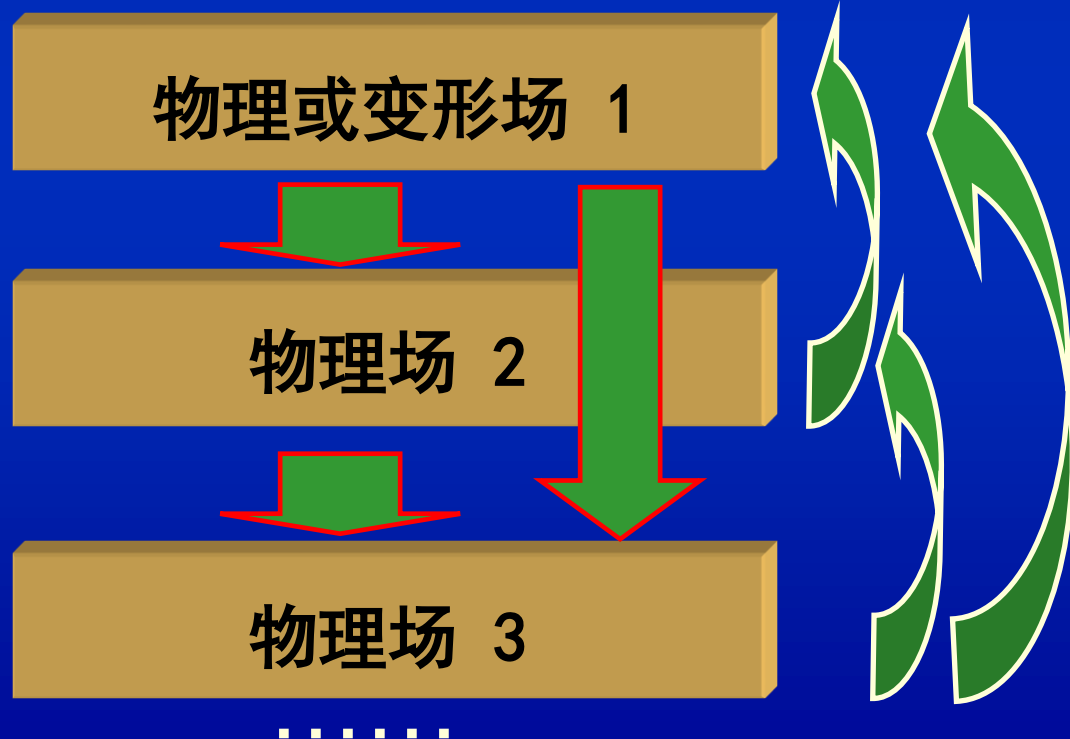
兰州大学
电磁固体力学研究组、
风沙物理研究组



耦合场分析方法

间接耦合 & 直接耦合方法

- **间接耦合方法**，或称**顺序耦合**、**序贯耦合方法**
按照顺序进行两次或更多次的相关场分析。



例：结构-热分析

温度场分析

热载荷

结构变形场分析



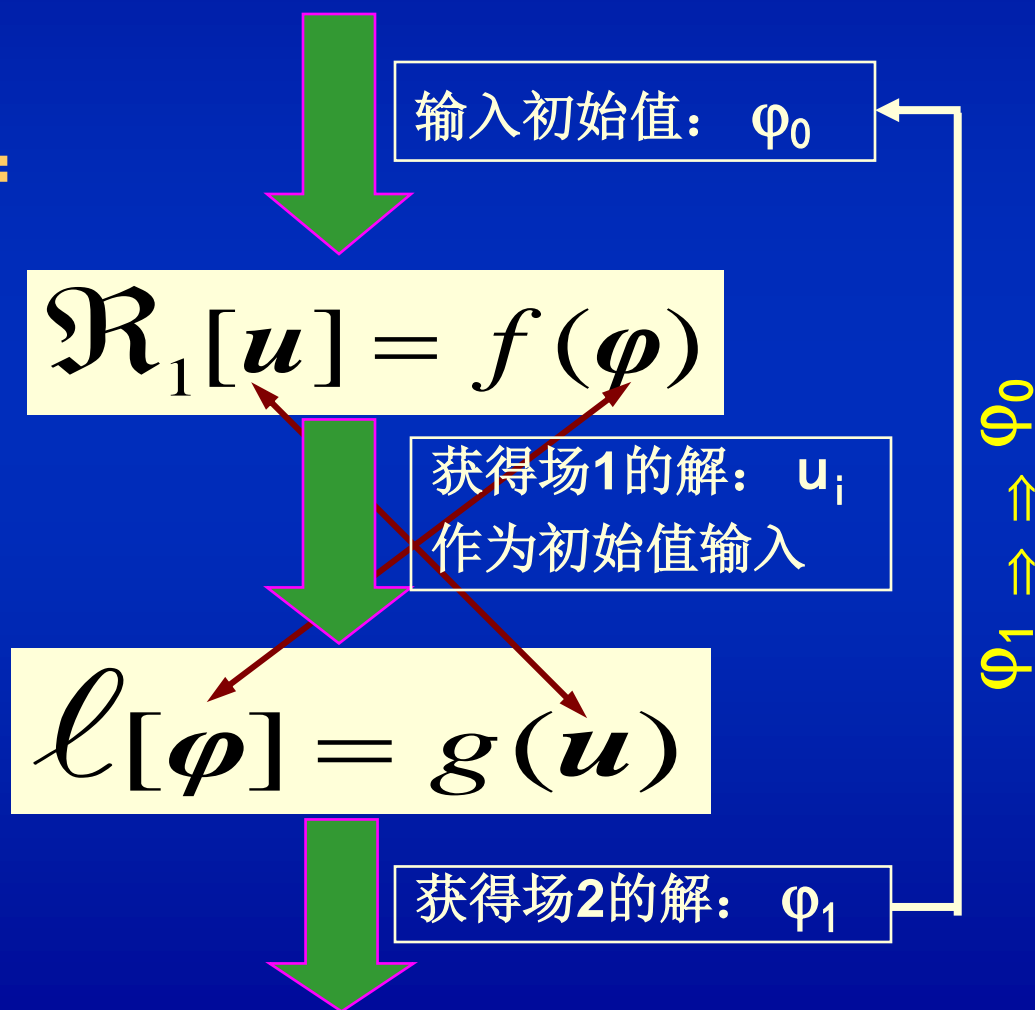
数学描述（以两个场耦合为例）

- 物理或力学变形场1:

场变量 u

- 物理或力学变形场2:

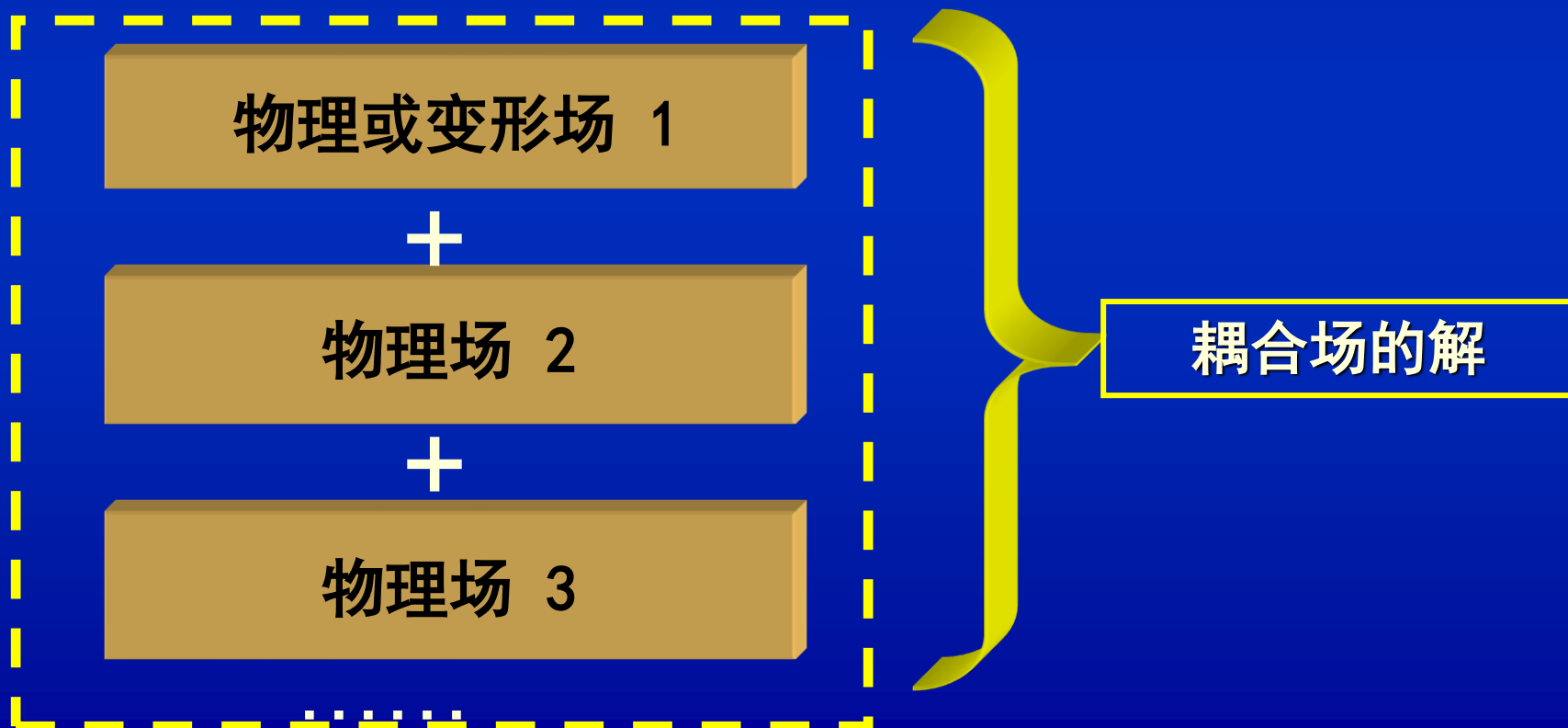
场变量 φ





● 直接耦合方法

两场或更多场的同时求解，以获得耦合场的解。





数学描述 (以两个场耦合为例)

➤ 物理或力学变形场1:
场变量 u

$$\mathcal{R}_1[u] = f(\varphi)$$

➤ 物理或力学变形场2:
场变量 φ

$$\mathcal{L}[\varphi] = g(u)$$

?

$$\mathcal{H} \begin{bmatrix} u \\ \varphi \end{bmatrix} = F(u, \varphi)$$

同时获得场变量: u 、 φ



两种耦合分析方法的比较

◆ 间接耦合方法

- ✓ 迭代思想
- ✓ 分场求解、方程阶数低
- ✓ 适合非线性程度不高的问题
- ✓ 每个场分析中均采用收敛条件
- ✓ 可能出现结果发散现象

理论上讲，不受问题限制，适合任何耦合场分析

◆ 直接耦合方法

- ✓ 逆算子思想
- ✓ “合场”求解、方程阶数高
- ✓ 适合高度非线性问题
- ✓ “合场”方程建立困难
- ✓ 高维非线性问题带来的困难

如：压电-结构耦合、流动-热传导耦合、电路-电磁场耦合等



耦合场的分析方法： —— 解耦方法

- 顺序求解各个物理场或者力学变形场，将获得了上一个场的相关信息后代入下一个场进行分析，最后获得多场作用下的总效果。
- 单向非双向、考虑作用但非相互作用与影响

✦ 并非真正的耦合，意义？

- 实际上我们熟悉了太多这样的问题：温度应力问题、早期的电磁结构变形分析、小变形、低温、低频、低电磁场下结构分析等...
- 可以给出一些解析解，可作为考虑耦合效应的考据
- 解耦单向分析思路考虑了双向的作用与影响就是顺序耦合思想



耦合问题的求解（间接、直接耦合分析）

● 解析、半解析求解耦合问题

- ✓ 主要适合解耦场分析、低维、低非线性
- ✓ 可在某些条件下的线性化问题分析中

● 数值求解耦合问题

- ✓ 目前的主要手段，适合多个场分析，稍高维、非线性
- ✓ 分为网格方法（有限元法、边界元法、有限差分法、有限体积法等）和无网格方法（再生核质子方法、有限点方法、MPLG法等）
- ✓ 数值仿真软件



- **商业软件：具有一定的耦合场分析功能**

- FEMLAB**：基于偏微分方程基础的软件，最新V3.2,可求解声场、扩散、电磁场、流体力学、结构力学问题或耦合问题；

- ANSYS**：最初为解决固体力学和结构力学问题，最新V10.0,陆续加入了对流场、声场、热场、电磁场的仿真功能，以及多场耦合的仿真算法；

- MSC. DYTRAN**：高度非线性、流体-结构耦合、瞬态动力响应问题仿真；

- ALGOR**：功能包括结构，流体，热，电磁分析以及目前主流有限元分析软件中最为便捷的多物理场耦合分析：流-固耦合分析和热-结构耦合分析，最新V14；

- ABQAS**：结构（应力/位移）问题，以及工程领域的热传导、质量扩散热电耦合分析、声学分析、岩土力学分析（流体渗透/应力耦合分析）及压电介质分析等。

- **开发耦合分析模块，或者商业软件的二次开发...**



一些耦合场分析实例

1. 力 - 磁、力 - 磁 - 热 耦合问题

- 区域耦合问题
- 解析解法
- 数值解法（有限元）间接耦合分析方法
- 多重非线性迭代技术



Background & Objective

❖ Applications:

Magnetic fusion, Energy storage device, Magnetohydrodynamic system (MHD), Magnetic forming, Magnetically levitated vehicles (MLV) ...

Magnetic guns or cannons in military field, Nuclear-magnetic-resonance measurement (NMR) for medical use ...

❖ Problems Induced & Objectives:

- ✓ **Stress in electromagnetic structures induced by electromagnetic forces**
- ✓ **Magneto-elastic stability**
- ✓ **Mechanics behaviour of electromagnetic structures under coupled multi-fields, such as magnetic, thermal, fluid fields and so on ...**



❖ Mathematic Modeling (板壳的力-磁变分理论, 多非线性) — Magnetoelastic generalized variational principle

(1) Magnetic energy of ME system (Magnetization nonlinearity)

$$\Pi^{em} \{ \phi, \mathbf{u} \} =$$

$$\int_{\Omega^+(\mathbf{u})} \left(\int_0^{H^+} B^+ dH^+ \right) dv + \frac{1}{2} \int_{\Omega^-(\mathbf{u})} \mu_0 (\nabla \phi^-)^2 dv + \int_{s_0} \mathbf{n} \cdot \mathbf{B}_0 \phi^- ds$$

(2) Strain energy of plate (Geometrical nonlinearity)

$$\begin{aligned} \Pi^{me} \{ \phi, \mathbf{u} \} = & \frac{1}{2} \int_{s^+} C \left[\frac{\partial u}{\partial x} + \frac{\partial v}{\partial y} + \frac{1}{2} (\bar{\nabla} w)^2 \right]^2 ds + \frac{1}{2} \int_{s^+} D (\bar{\nabla}^2 w)^2 ds \\ & + \int_{s^+} C(1-\nu) \left\{ \frac{1}{4} \left[\frac{\partial u}{\partial y} + \frac{\partial v}{\partial x} + \frac{\partial w}{\partial x} \frac{\partial w}{\partial y} \right]^2 - \left[\frac{\partial u}{\partial x} + \frac{1}{2} \left(\frac{\partial w}{\partial x} \right)^2 \right] \left[\frac{\partial v}{\partial y} + \frac{1}{2} \left(\frac{\partial w}{\partial y} \right)^2 \right] \right\} ds \\ & + \int_{s^+} D(1-\nu) \left[\left(\frac{\partial^2 w}{\partial x \partial y} \right)^2 - \frac{\partial^2 w}{\partial x^2} \frac{\partial^2 w}{\partial y^2} \right] ds \end{aligned}$$

(3) Total generalized energy of ME system

$$\Pi \{ \phi, \mathbf{u} \} = \Pi^{em} \{ \phi, \mathbf{u} \} + \Pi^{me} \{ \phi, \mathbf{u} \}$$



(4) Magnetoelastic generalized variational principle

$$\delta \Pi \{ \phi, \mathbf{u} \} = \delta_{\phi} \Pi \{ \phi, \mathbf{u} \} + \delta_{\mathbf{u}} \Pi \{ \phi, \mathbf{u} \} = 0$$

Magnetic Field

Governing equations
& Boundary conditions

Mechanics Deformation Field

Governing equations &
Boundary conditions for plates

(5) Equivalent magnetic forces exerted on SFM plates

$$q_z^{em}(x, y) = \left[\frac{\mu_m^2}{2\mu_0} (\mathbf{H}_n^+)^2 + \frac{\mu_0}{2} (\mathbf{H}_\tau^+)^2 - \int_0^{H^+} B^+ dH^+ \right]_{z=-h/2}^{z=h/2}$$

Explanation:

Transformation from
the magnetic energy
to the mechanical energy
of the system.



❖ Numerical Method -- Coupled FEM for Multi-fields

Magnetic Field

FEM for Magnetic Field

$$[\mathbf{K}^{em}([\Phi], [\mathbf{U}]][\Phi] = [\mathbf{P}]$$

N-R Method for nonlinearity of MF

$$[\Phi_{m+1}] = [\Phi_m] - [\mathbf{J}_m]^{-1} \{ [\mathbf{K}_m^{em}([\mathbf{U}^*], [\Phi_m])][\Phi_m] - [\mathbf{P}] \}$$

Mechanics

Deformation Field

FEM for Deformation Field

$$[\mathbf{K}^{me}([\mathbf{U}]][\mathbf{U}] = [\mathbf{Q}([\Phi([\mathbf{U}])])]$$

N-R Method for nonlinearity of MDF

$$[\mathbf{U}_{n+1}] = [\mathbf{U}_n] - [\mathbf{A}_n]^{-1} \{ [\mathbf{K}_n^{me}([\mathbf{U}_n])][\mathbf{U}_n] - [\mathbf{Q}([\Phi^*([\mathbf{U}_n])])] \}$$

Iteration Method for nonlinearity of coupling fields: $\| \mathbf{U}_{m,n+1} - \mathbf{U}_{m,n} \| < \delta$

Solutions

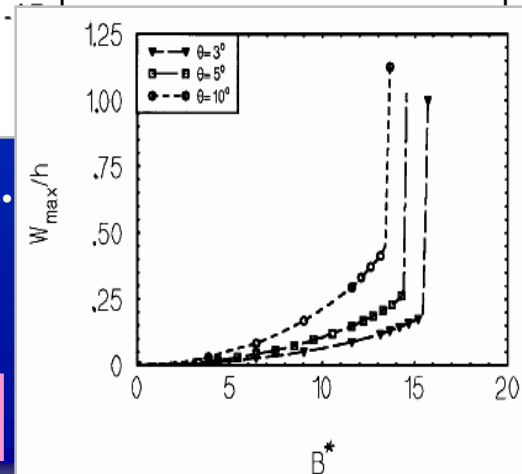
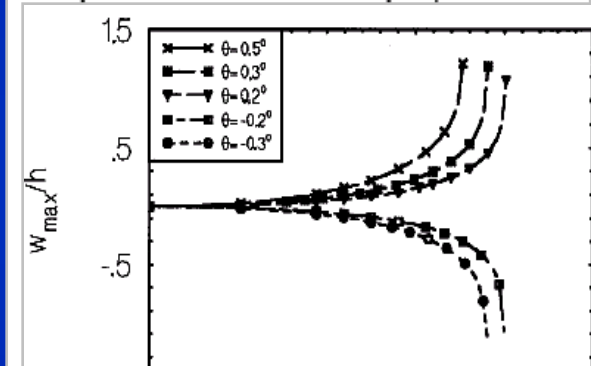
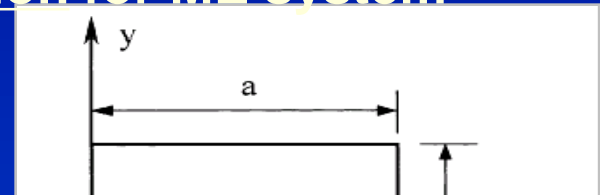


❖ Numerical Simulation Results

(1) Linear magnetization and linear deformation for ME system

TABLE 1. Comparison of Critical Magnetic Fields $B_{cr}^* [=B_{cr}/(\mu_0 E)^{1/2} \times 10^4]$

a (cm) (1)	b (cm) (2)	h (cm) (3)	Experiment of Miya et al. (1980) (4)	Theoretical Results (Error in %)	
				Moon et al. (1968) (5)	This paper (6)
10	1	0.04	1.03	1.07 (3.9)	1.08 (4.9)
15	1	0.12	2.31	3.01 (30.3)	2.32 (0.4)
10	1	0.12	4.06	5.54 (36.3)	4.25 (4.7)
15	1	0.16	2.91	4.64 (59.5)	3.08 (5.8)
10	1	0.16	5.48	8.83 (61.1)	5.90 (7.7)
15	1	0.20	3.89	6.49 (66.8)	4.09 (5.1)
10	1	0.20	7.02	11.9 (69.5)	7.34 (4.6)
15	1	0.25	5.02	9.06 (80.5)	5.46 (8.8)
10	1	0.25	9.27	16.7 (79.8)	9.81 (5.6)

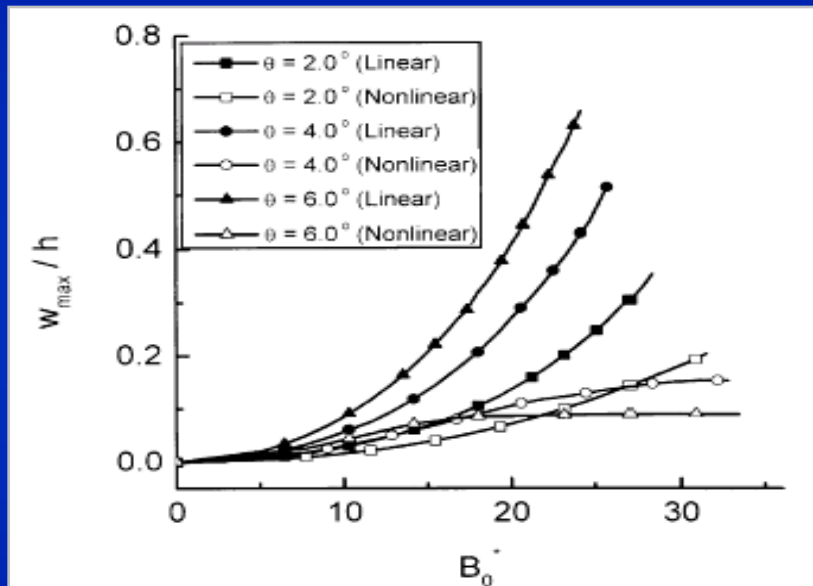


Note: i) For cantilevered SFM plate in transverse magnetic field.
ii) Edge effect of magnetic field included.

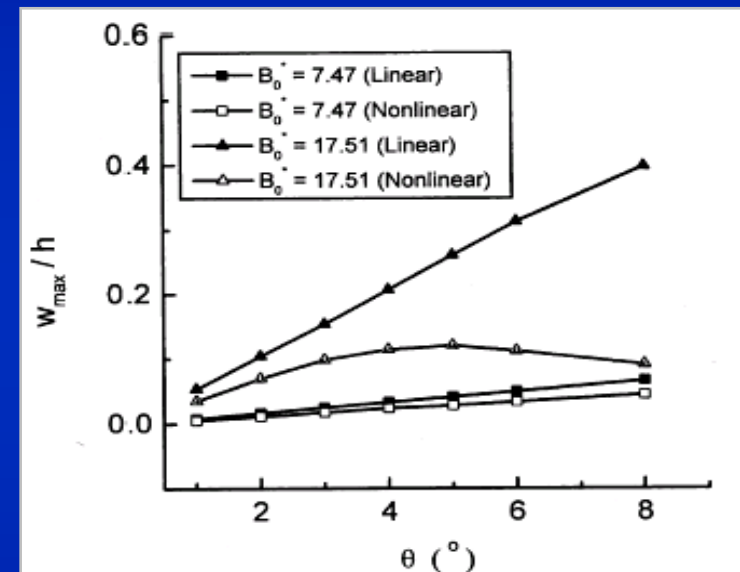
Zheng XJ, Zhou YH, Wang X, et al ASCE J. Eng. Mech. 1999



(2) Nonlinear magnetization and linear deformation for ME system



SFM simply supported plate in oblique magnetic field: W_{\max} vs. B_0 .

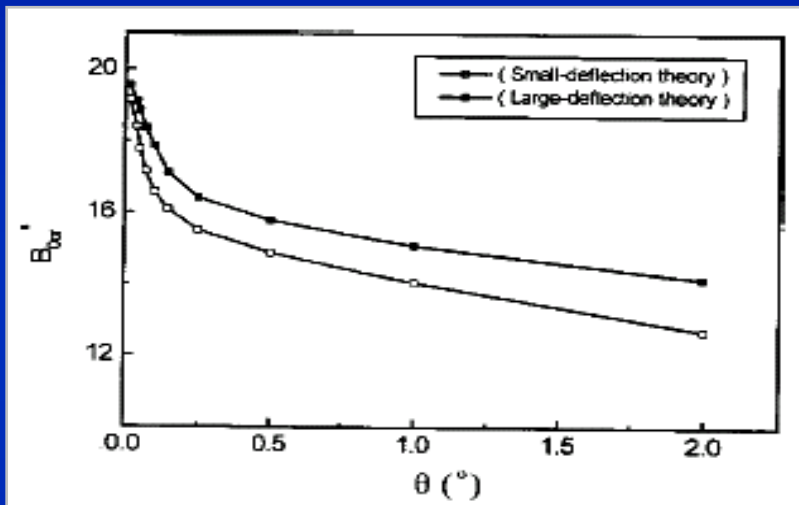


SFM simply supported plate in oblique magnetic field: W_{\max} vs. θ .

Zheng XJ, Wang X, *INT. J. Solids Struct.* 2001

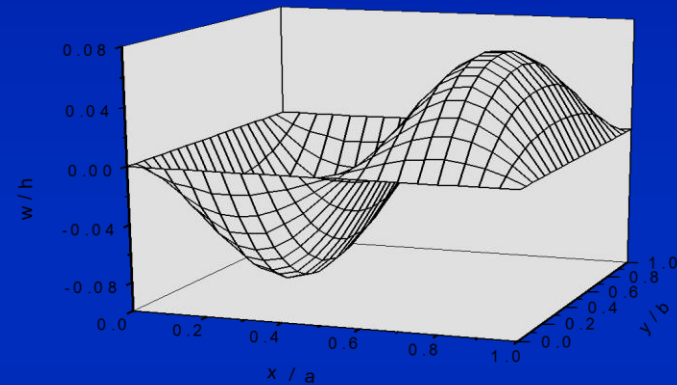


(3) Linear magnetization and nonlinear deformation for ME system

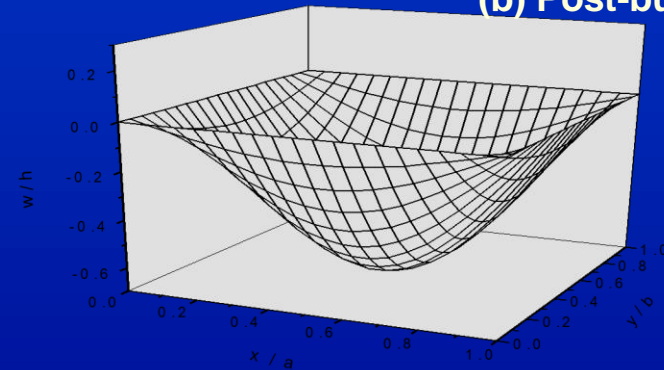


Effect of incident angle θ on B_{0cr} for SFM cantilevered plate

(a) Pre-buckling



(b) Post-buckling



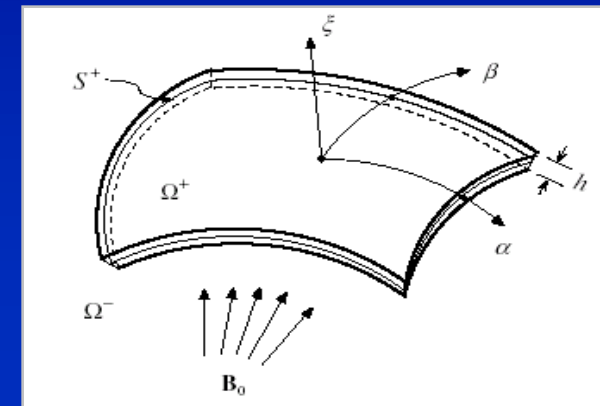
Zheng XJ, Wang X, *ASCE J. Eng. Mech.* 2003



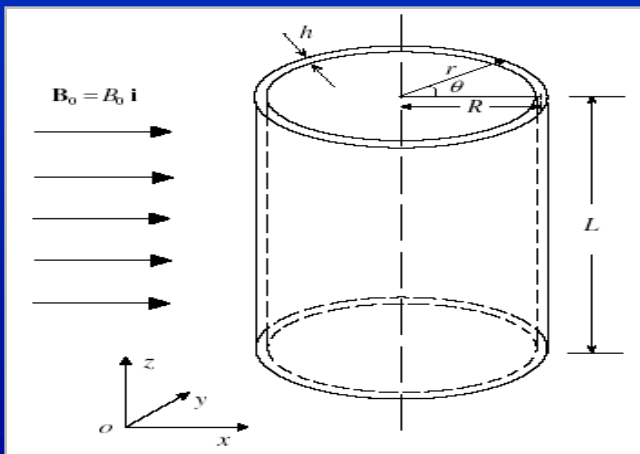
(4) Mathematic Modeling and simulation For SFM Shells

Strain energy of shell

$$\Pi^{me} \{ \phi, \mathbf{u} \} = \frac{1}{2} \int_{S^+} \left\{ C [\varepsilon_\alpha^2 + \varepsilon_\beta^2 + 2\nu \varepsilon_\alpha \varepsilon_\beta + \frac{1}{2} (1-\nu) \varepsilon_{\alpha\beta}^2] \right. \\ \left. + D [\chi_\alpha^2 + \chi_\beta^2 + 2\nu \chi_\alpha \chi_\beta + (1-\nu) \chi_{\alpha\beta}^2] \right\} ds$$



对已有实验的模拟



数值模型

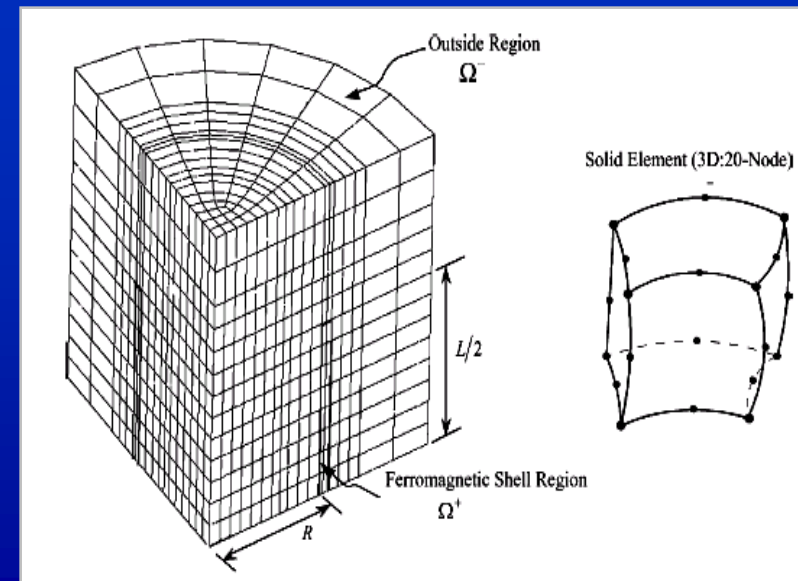
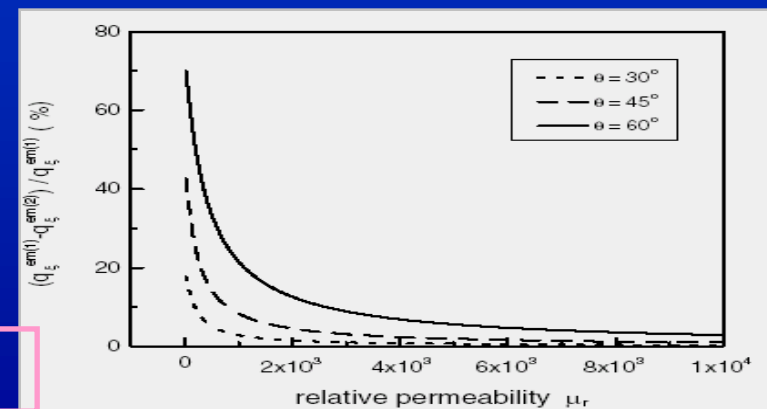
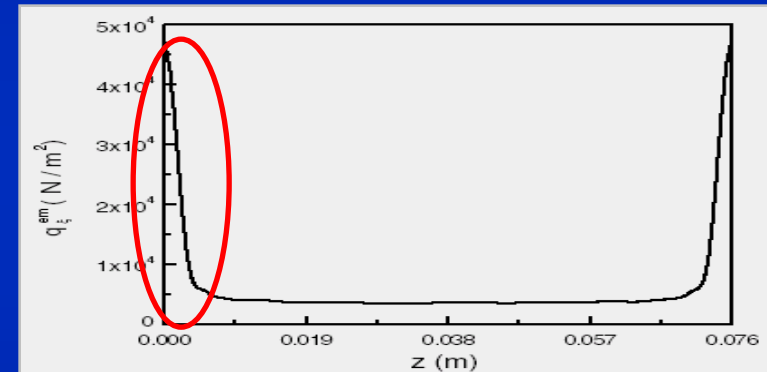
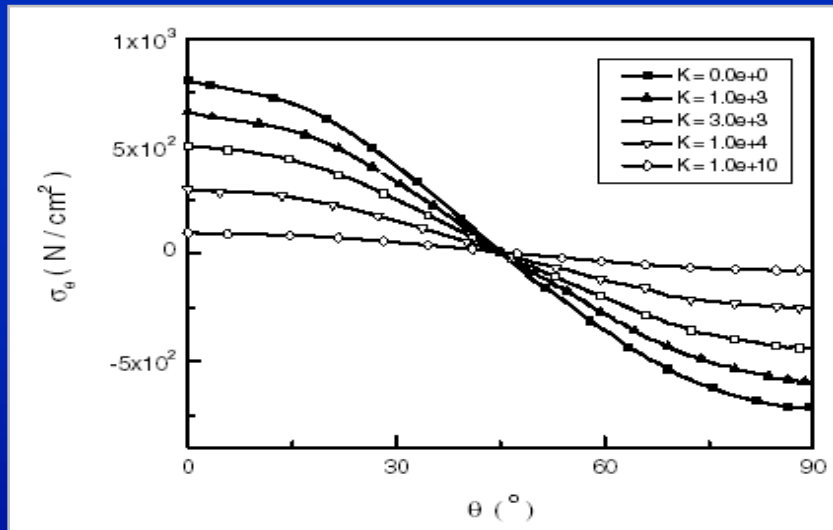




Table 2

The circumferential strain at the middle section of a ferromagnetic cylindrical shell in magnetic field ($B_0 = 1.0$ T)

Strain $\varepsilon_\theta (\times 10^{-6})$	Experiment result Miyata and Miya (1988)	This paper result	Moon and Pao (1968)	Pao and Yeh (1973)	Eringen and Maugin (1990)
$\theta = 0^\circ$	250	306	531	397	489
Relative error (%)	-	(22.4)	(112.4)	(58.5)	(95.6)
$\theta = 90^\circ$	-152	-175	-576	-203	-7134
Relative error (%)	-	(15.1)	(278.9)	(33.6)	(4593.4)



Zheng XJ, Wang X, *INT. J. Solids Struct.* 2003



❖ Mathematic Modeling (广义磁热弹性变分理论)

— Magneto-thermo-elastic generalized variational principle

(1) Magnetic energy of MTE system (Magnetization nonlinearity)

$$\Pi^{em} \{ \phi, \mathbf{u} \} =$$

$$\int_{\Omega^+(\mathbf{u})} \left(\int_0^{H^+} B^+ dH^+ \right) dv + \frac{1}{2} \int_{\Omega^-(\mathbf{u})} \mu_0 (\nabla \phi^-)^2 dv + \int_{S_0} \mathbf{n} \cdot \mathbf{B}_0 \phi^- ds$$

(2) Total mechanical energy of thermoelasticity for MTE system

$$\begin{aligned} \Pi^{me} \{ \mathbf{u}, T \} &= \int_{\Omega^+} [\Sigma(\mathbf{e}, T) + \eta_T T - \mathbf{f}^{me} \cdot \mathbf{u}] dv - \int_{S_t} \mathbf{F}^{me} \cdot \mathbf{u} ds \\ &= \int_{\Omega^+} \left\{ \frac{1}{2} \lambda [tr(\mathbf{e})]^2 + \mathbf{G} \mathbf{e} : \mathbf{e} - \alpha (3\lambda + 2G) [tr(\mathbf{e})] (T - T_0) \right. \\ &\quad \left. - \frac{C_E (T - T_0)^2}{2T_0} + \eta_T T - \mathbf{f}^{me} \cdot \mathbf{u} \right\} dv - \int_{S_t} \mathbf{F}^{me} \cdot \mathbf{u} ds \end{aligned}$$



(3) Heat potential energy of thermal flux of MTE system

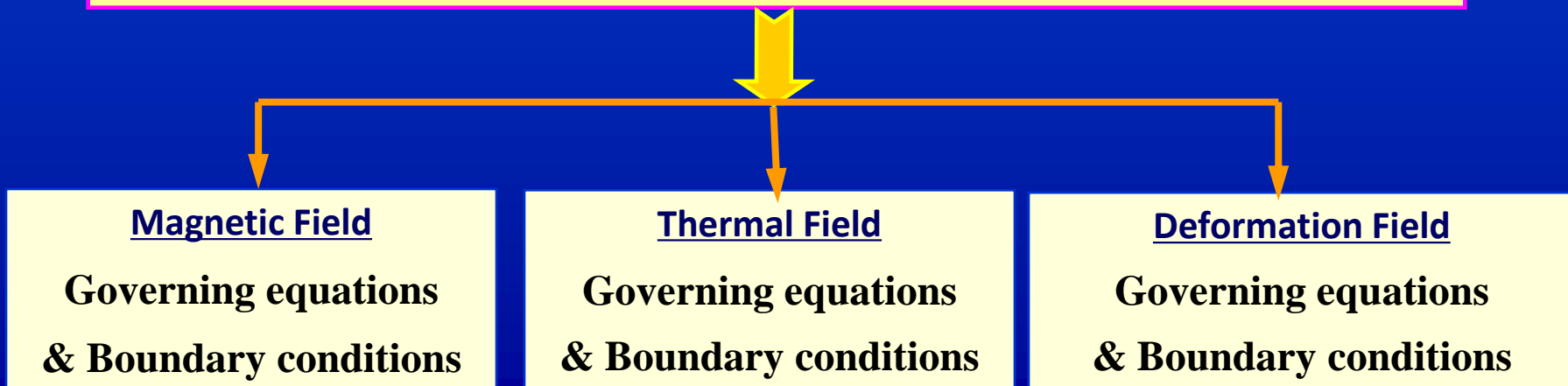
$$\Pi^{th}\{T\} = \int_{\Omega^+} \left[\frac{1}{2} k (\nabla T)^2 - \rho h_T T \right] dv - \int_{S_p} \left[(\lambda_1 \bar{q} - \lambda_2 H_T \bar{T}) T - \frac{1}{2} \lambda_2 H_T T^2 \right] ds$$

(4) Functional of total generalized energy of MTE system

$$\Pi\{\phi, \mathbf{u}, T\} = \Pi^{em}\{\phi, \mathbf{u}\} + \Pi^{me}\{\mathbf{u}, T\} + \Pi^{th}\{T\}$$

(5) Magneto-thermo-elastic generalized variational principle

$$\delta \Pi\{\phi, \mathbf{u}, T\} = \delta_\phi \Pi\{\phi, \mathbf{u}, T\} + \delta_{\mathbf{u}} \Pi\{\phi, \mathbf{u}, T\} + \delta_T \Pi\{\phi, \mathbf{u}, T\} = 0$$





❖ Analysis (Magneto-thermo-elastic buckling of SFM plate)

—— 解析分析磁热弹性板的屈曲问题

➤ Equations

$\delta\phi$: Equations for magnetic field;

δT : Equations for thermal field;

δw : Bending equation of plate:

$$q_z^{em}(x,y) = \frac{\mu_0 \lambda \mu_r}{2} \left\{ [H_n^+(x,y,h/2)]^2 - [H_n^+(x,y,-h/2)]^2 \right\} - \frac{\mu_0 \lambda}{2} \left\{ [H_\tau^+(x,y,h/2)]^2 - [H_\tau^+(x,y,-h/2)]^2 \right\}$$

$$\nabla \cdot (\mu \nabla \phi^+) = 0 \quad \text{in } \Omega^+(\mathbf{u})$$

$$\nabla^2 \phi^- = 0 \quad \text{in } \Omega^-(\mathbf{u})$$

$$\phi^+ = \phi^-, \quad \mu \frac{\partial \phi^+}{\partial n} = \mu_0 \frac{\partial \phi^-}{\partial n} \quad \text{on } S$$

$$-\nabla \phi^- = \frac{\mathbf{B}_0}{\mu_0} \quad \text{on } \Gamma_0 \text{ or at } \infty$$

$$k \nabla^2 T + \rho h_T = 0 \quad \text{in } \Omega^+$$

$$T = T^* \quad \text{on } S_T$$

$$k \frac{\partial T}{\partial n} = \lambda_1 \bar{q} + \lambda_2 H_T (T - \bar{T}) \quad \text{on } S_P$$

$$D \bar{\nabla}^2 \bar{\nabla}^2 w + \frac{\alpha E}{1-\nu} \int_{-h/2}^{h/2} \bar{\nabla}^2 (T - T_0) z dz - \left(N_x \frac{\partial^2 w}{\partial x^2} + 2N_{xy} \frac{\partial^2 w}{\partial x \partial y} + N_y \frac{\partial^2 w}{\partial y^2} \right) = q_z^{em}(x,y)$$



➤ Solutions

For simply supported rectangular SFM plates (without edge effect)

$$w = \sum_m \sum_n A_{mn} \sin \frac{m\pi x}{a} \sin \frac{n\pi y}{b}$$

$$\mathbf{H}^+ = \mathbf{H}_0^+ + \mathbf{h}^+ = -\nabla\Phi^+ - \nabla\phi^+ \quad \text{in } \Omega^+(\mathbf{u})$$

$$\mathbf{H}^- = \mathbf{H}_0^- + \mathbf{h}^- = -\nabla\Phi^- - \nabla\phi^- \quad \text{in } \Omega^-(\mathbf{u})$$

线性化、摄动理论

$$\mathbf{H}_0^+ = -\nabla\Phi^+ = B_0/\mu_0\mu_r \mathbf{k} \quad \text{in } \Omega^+(\mathbf{u} \equiv 0)$$

$$\mathbf{H}_0^- = -\nabla\Phi^- = B_0/\mu_0 \mathbf{k} \quad \text{in } \Omega^-(\mathbf{u} \equiv 0)$$

磁场

温度场

结构变形场

$$\mathbf{h}^+ = -\nabla\phi^+$$

$$= \frac{B_0\chi}{\mu_0\mu_r} \sum_m \sum_n \frac{A_{mn}}{\Delta_{mn}} \frac{m\pi}{a} \cos \frac{m\pi x}{a} \sin \frac{n\pi y}{b} \cosh(k_{mn}z) \mathbf{i} + \frac{B_0\chi}{\mu_0\mu_r} \sum_m \sum_n \frac{A_{mn}}{\Delta_{mn}} \frac{n\pi}{b} \sin \frac{m\pi x}{a} \times \cos \frac{n\pi y}{b} \cosh(k_{mn}z) \mathbf{j} + \frac{B_0\chi}{\mu_0\mu_r} \sum_m \sum_n \frac{A_{mn}k_{mn}}{\Delta_{mn}} \sin \frac{m\pi x}{a} \sin \frac{n\pi y}{b} \sinh(k_{mn}z) \mathbf{k}$$

$$\mathbf{h}^- = -\nabla\phi^-$$

$$= -\frac{B_0\chi}{\mu_0} \sum_m \sum_n \frac{A_{mn}}{\Delta_{mn}} \frac{m\pi}{a} \cos \frac{m\pi x}{a} \sin \frac{n\pi y}{b} \sinh\left(\frac{k_{mn}h}{2}\right) e^{k_{mn}(h/2-|z|)} \mathbf{i} \\ - \frac{B_0\chi}{\mu_0} \sum_m \sum_n \frac{A_{mn}}{\Delta_{mn}} \frac{n\pi}{b} \sin \frac{m\pi x}{a} \cos \frac{n\pi y}{b} \sinh\left(\frac{k_{mn}h}{2}\right) e^{k_{mn}(h/2-|z|)} \mathbf{j} \\ - \frac{B_0\chi}{\mu_0} \operatorname{sgn}(z) \sum_m \sum_n \frac{A_{mn}k_{mn}}{\Delta_{mn}} \sin \frac{m\pi x}{a} \sin \frac{n\pi y}{b} \sinh\left(\frac{k_{mn}h}{2}\right) e^{k_{mn}(h/2-|z|)} \mathbf{k}$$



$$\sum_m \sum_n A_{mn} \left[Dk_{mn}^4 - \frac{2B_0^2 \chi^2 k_{mn}}{\mu_0 \mu_r \Delta_{mn}} \sinh \frac{k_{mn} h}{2} - \frac{\alpha Y T h}{1 - \nu} k_{mn}^2 \right] \sin \frac{m\pi x}{a} \sin \frac{n\pi y}{b} = 0$$

$$Dk_{mn}^4 - \frac{2B_{0mn}^2 \chi^2 k_{mn}}{\mu_0 \mu_r \Delta_{mn}} \sinh \frac{k_{mn} h}{2} - \frac{\alpha Y T_{mn} h}{1 - \nu} k_{mn}^2 = 0$$

➤ Buckling

Case (i). Magneto-elasticity:

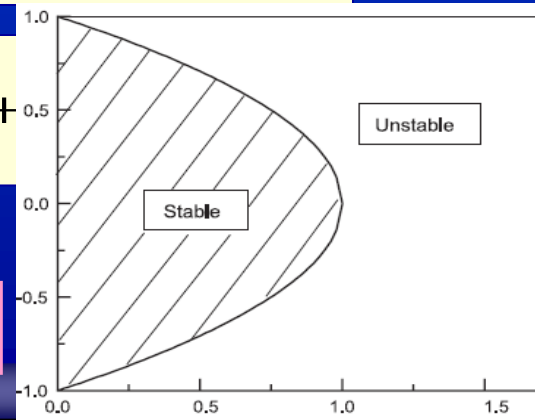
$$B_{cr}^* = \frac{B_{0cr}}{\sqrt{\mu_0 Y}} = \frac{\pi}{2} \left[\frac{\pi}{6(1-\nu^2)} \right]^{1/2} [1 + (a/b)^2]^{3/4} (a/h)^{-3/2}$$

Case (ii). Thermo-elasticity:

$$T_{cr}^* = \alpha T_{cr} = \frac{\pi^2}{12(1+\nu)} [1 + (a/b)^2] (a/h)^{-2}$$

Case (iii). Magneto-thermo-elasticity:

$$\left(\frac{B^*}{B_{cr}^*} \right)^2 +$$





❖ Simulations — For rectangular SFM plates (with edge effect)

$$\Pi_{em}\{\phi, \mathbf{u}\} = \frac{1}{2} \int_{\Omega^+(\mathbf{u})} \mu_0 \mu_r (\nabla \phi^+)^2 dv + \frac{1}{2} \int_{\Omega^-(\mathbf{u})} \mu_0 (\nabla \phi^-)^2 dv + \int_{S_0} \mathbf{n} \cdot \mathbf{B}_0 \phi^- ds$$

$$\Pi_{me}\{\phi, \mathbf{u}\} = \Pi_{me}^1 + \Pi_{me}^2 + \Pi_{me}^3$$

+

$$\Pi_{me}^1 = \frac{1}{2} \int_{S^+} C [(\varepsilon_x + \varepsilon_y)^2 + 2(1 - \nu)(\varepsilon_{xy}^2 - \varepsilon_x \varepsilon_y)] ds$$

$$\Pi_{me}^2 = \frac{1}{2} \int_{S^+} D [(\chi_x + \chi_y)^2 + 2(1 - \nu)(\chi_{xy}^2 - \chi_x \chi_y)] ds$$

$$\begin{aligned} \Pi_{me}^3 = & -\frac{\alpha Y}{1 - \nu} \int_{S^+} (\varepsilon_x + \varepsilon_y) \left[\int_{-h/2}^{h/2} (T - T_0) dz \right] ds + \frac{\alpha Y}{1 - \nu} \int_{S^+} (\chi_x + \chi_y) \left[\int_{-h/2}^{h/2} (T - T_0) z dz \right] ds \\ & - \left[\frac{C_E}{2T_0} + \frac{\alpha^2 Y (1 + \nu)}{(1 - \nu)(1 - 2\nu)} \right] \int_{S^+} \int_{-h/2}^{h/2} (T - T_0)^2 dz ds \end{aligned}$$

$$\Pi\{\phi, \mathbf{u}\} = \Pi_{em}\{\phi, \mathbf{u}\} + \Pi_{me}\{\phi, \mathbf{u}\}$$

磁场

$$\frac{\partial N_x}{\partial x} + \frac{\partial N_{xy}}{\partial y} = 0, \quad \frac{\partial N_{xy}}{\partial x} + \frac{\partial N_y}{\partial y} = 0$$

$$D \nabla^2 \nabla^2 w + \frac{\alpha Y}{1 - \nu} \int_{-h/2}^{h/2} \nabla^2 (T - T_0) z dz - \left(N_x \frac{\partial^2 w}{\partial x^2} + 2N_{xy} \frac{\partial^2 w}{\partial x \partial y} + N_y \frac{\partial^2 w}{\partial y^2} \right) = q_z^{em}(x, y, T)$$



$$\Pi_{th}\{T\} = \int_{\Omega^+} \left[\frac{1}{2}k(\nabla T)^2 - \rho h_T T \right] dv - \int_{S_P} \left[(\lambda_1 \bar{q} - \lambda_2 H_T \bar{T})T - \frac{1}{2}\lambda_2 H_T T^2 \right] ds$$

$$\nabla^2 T + \rho h_T = 0 \quad \text{in } \Omega^+$$

$$k \frac{\partial T}{\partial n} = \lambda_1 \bar{q} + \lambda_2 H_T (T - \bar{T}) \quad \text{on } S_P$$

FEM formulation for magnetic field

$$[\mathbf{K}^{em}][\Phi] = [\mathbf{P}] \quad [\mathbf{K}^{em}] = [\mathbf{K}^{em}(\mathbf{u}, T)]$$

FEM formulation for thermal field

$$[\mathbf{K}^{th}(\mathbf{u})][\mathbf{T}] = [\mathbf{Q}(\mathbf{u})]$$

FEM formulation for plate

$$[\mathbf{K}^{me}][\mathbf{U}] = [\mathbf{R}]$$

$$[\mathbf{K}^{me}] = [\mathbf{K}^{me}([\mathbf{U}])], \quad [\mathbf{R}] = [\mathbf{R}([\Phi([\mathbf{U}])])]$$



Iterative method

$$(1) \quad [\mathbf{U}_{m+1}] = [\mathbf{U}_m] - [\bar{\mathbf{K}}_m^{me}]^{-1} [\Psi([\mathbf{U}_m])]$$

$$(2) \quad [\Psi([\mathbf{U}_m])] = [\mathbf{K}^{me}([\mathbf{U}_m])][\mathbf{U}_m] - [\mathbf{R}([\mathbf{K}^{em}([\mathbf{U}_m])]^{-1}[\mathbf{P}], T)]$$

$$(3) \quad [\Psi([\mathbf{U}_m^{n+1,n}])] = [\mathbf{K}^{me}([\mathbf{U}_m^{n+1}])][\mathbf{U}_m^{n+1}] - [\mathbf{R}([\mathbf{K}^{em}([\mathbf{U}_m^n])]^{-1}[\mathbf{P}], T)]$$

$$(4) \quad [\mathbf{U}_{m+1}^{n+1}] = [\mathbf{U}_m^{n+1}] - [\bar{\mathbf{K}}_m^{me}]_{n+1,n}^{-1} [\Psi([\mathbf{U}_m^{n+1,n}])]$$

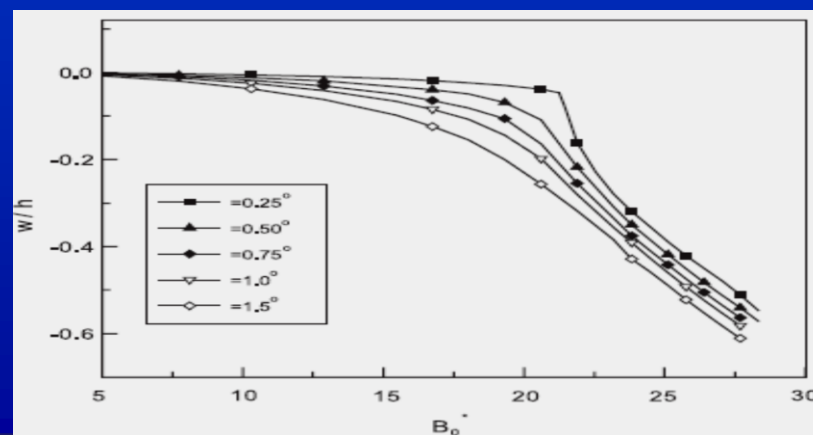
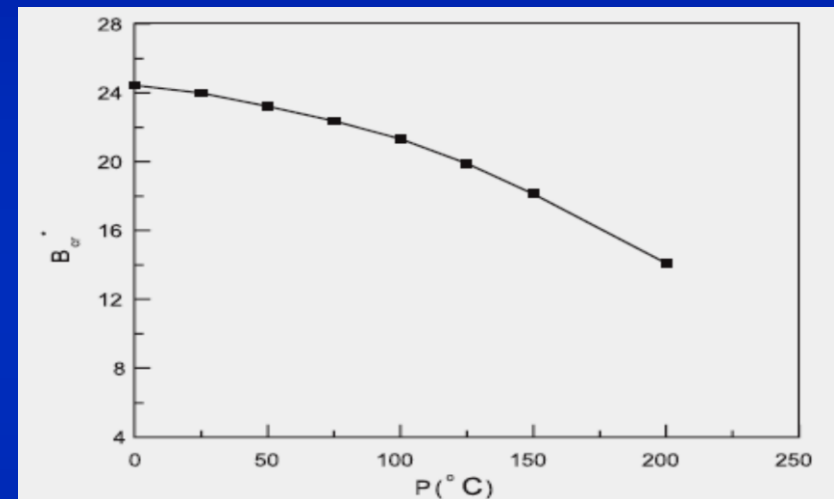
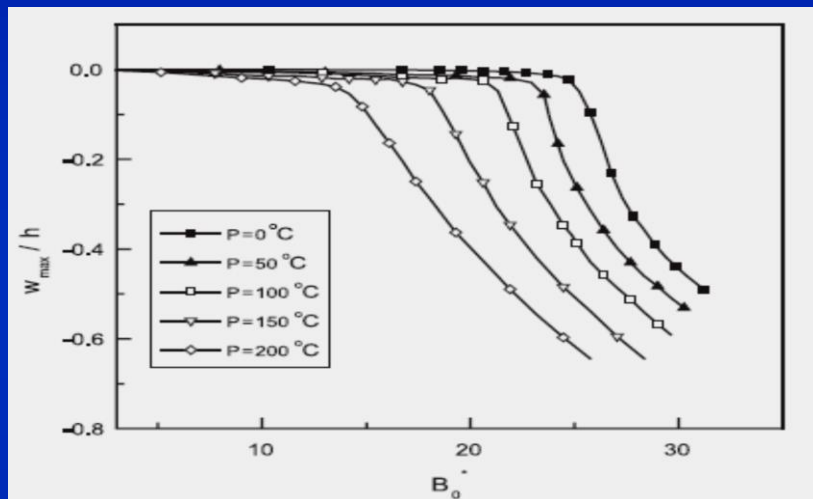
Repeat (1)~(4), until the following conditions

$$(5) \quad \|\Psi([\mathbf{U}_m^{n+1,n}])\| < \varepsilon_1, \quad \|[\mathbf{U}_{m+1}^{n+1}] - [\mathbf{U}_m^{n+1}]\| < \varepsilon_2$$



$$T = P \cos(\pi y/b), \quad \text{at } x = 0; \quad T = 0, \quad \text{at } x = a$$

$$\partial T / \partial y = 0, \quad \text{at } y = 0, b$$





$$T = T_0 + \delta T, \quad \text{at } z = h/2; \quad T = T_0, \quad \text{at } z = -h/2$$

$$k \partial T / \partial y = H_T (T - T_0), \quad \text{at } x = 0, a \text{ and } y = 0, b$$

(a) $B = \mu_0 \mu_r H$ with $\mu_r = 1000$, and (b) $B = \mu_0 \mu_r(T) H$ with $\mu_r(T) = \beta_1 + \beta_2 T$.

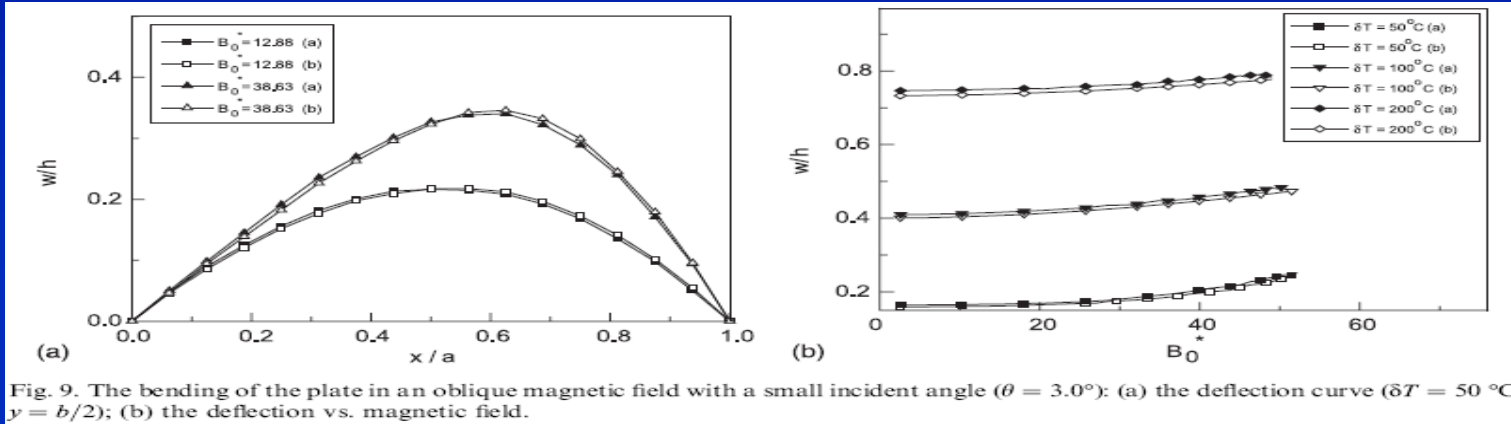


Fig. 9. The bending of the plate in an oblique magnetic field with a small incident angle ($\theta = 3.0^\circ$): (a) the deflection curve ($\delta T = 50^\circ\text{C}$, $y = b/2$); (b) the deflection vs. magnetic field.

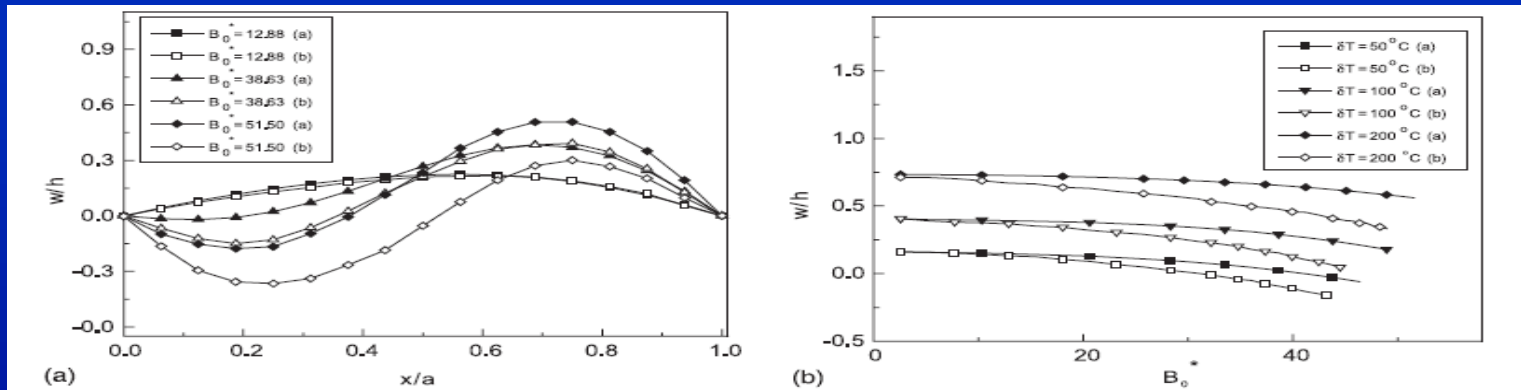


Fig. 10. The bending of the plate in an oblique magnetic field with a large incident angle ($\theta = 10.0^\circ$): (a) the deflection curve ($\delta T = 50^\circ\text{C}$, $y = b/2$); (b) the deflection vs. magnetic field.



一些耦合场分析实例

2. 力 - 磁耦合动力学问题

- 力-磁耦合动力学模型与数值分析
- 复杂动力学行为:非线性、磁阻尼、混沌
-

1. Xingzhe Wang, et al. *ASCE Journal of Engineering Mechanics*, 2006, 132(4):422-428
2. Xingzhe Wang, et al. *Int J of Mechanical Sciences*, 2006,48(8):889-898
3. Xingzhe Wang, *Int Conference on enhancement and promotion of Computational Methods in Engineering Science and Mechanics*, 2006, Aug, Changchun, China



一些耦合场分析实例

3. 空气-弹性、空气-弹性-控制 耦合问题

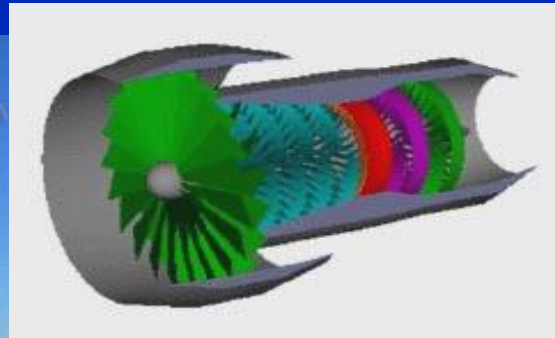
- 边界耦合问题
- 半解析半数值解法



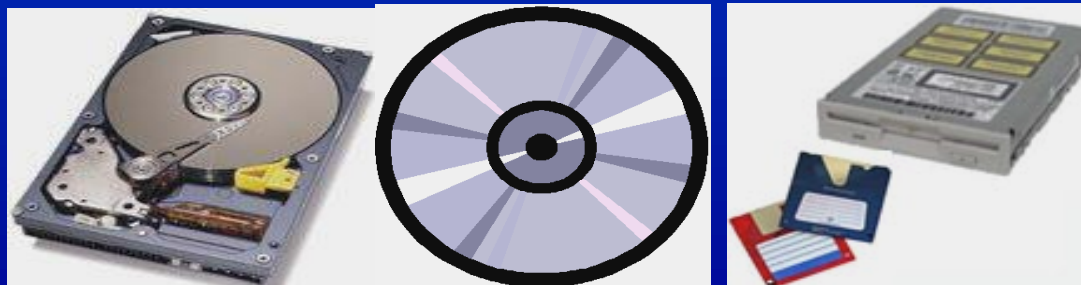
Background & Objective

□ 应用背景:

- Flexible rotating blades, gas turbines, circular saws

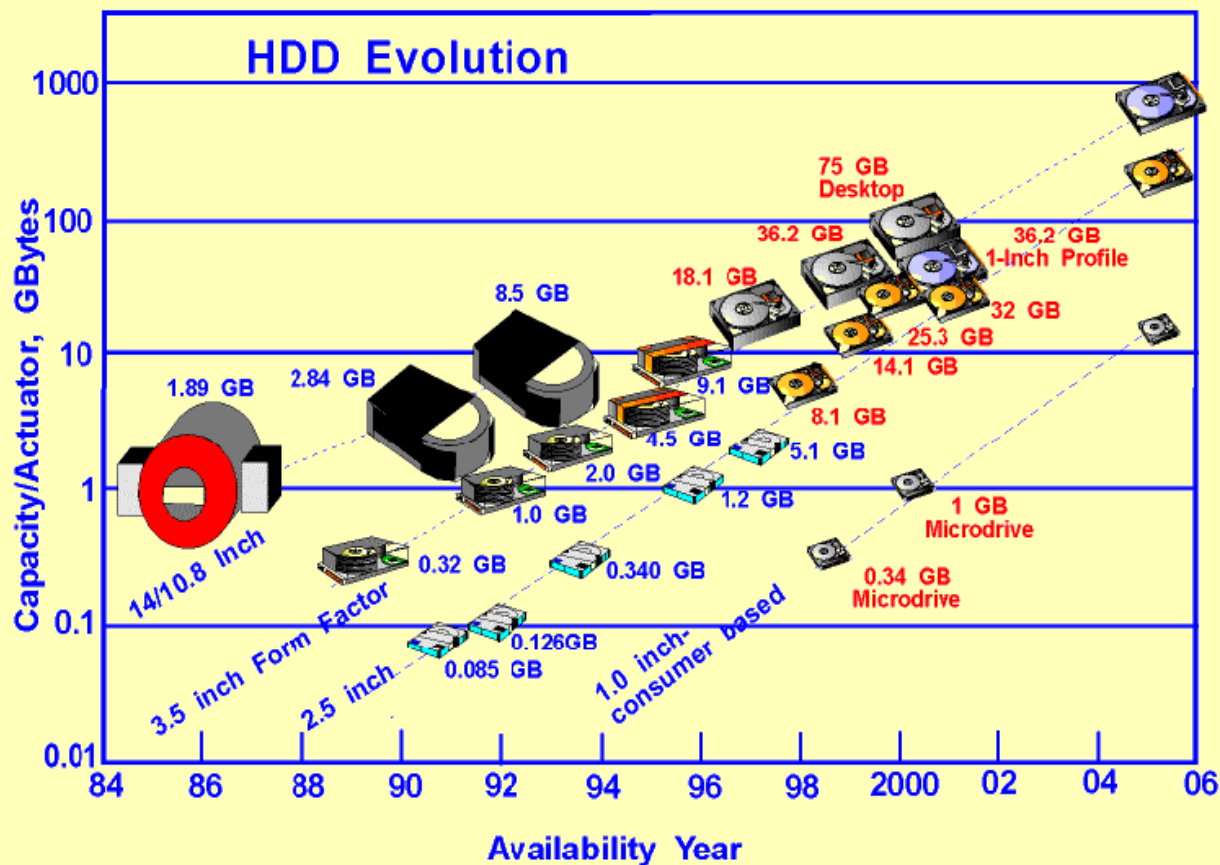


- High density and high speed —
HDD, VCD/DVD, Floppy Disk.





➤ 现代高密磁盘发展



✓容量(磁盘密度):

增长了25M倍,

100%/每年

✓驱动电机:

几百转/分钟→

7500转/分钟→上万

✓尺寸:

24英寸→1.0英寸

✓盘片:

24片→2-3片、单片



➤ 磁盘工业与设计(HDD)的力学问题

磁头悬臂的振动、动力稳定性;

读写磁头的悬浮、定位与控制;

磁记录介质表面摩擦学;

磁盘的噪声与控制;

高速旋转磁盘空气弹性失稳——颤振, 及其控制.

旋转振动圆盘具有稳定性:

1) 屈曲失稳(行波频率之一
等于零)

2) 颤振失稳(负阻尼)

❖ Rotating Disk Flutter (颤振) ?

Hydrodynamic instability caused by aeroelastic coupling between rotating disk and surrounding airflow.

Critical speed for disk flutter

——Flutter Speed (临界旋转速度)



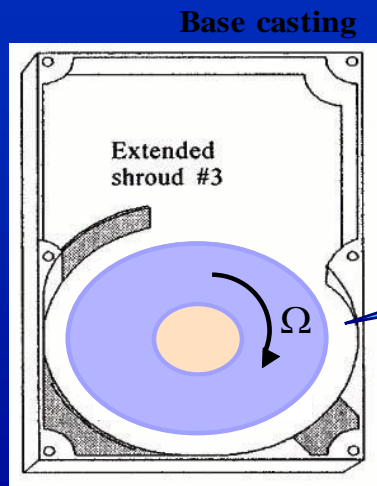
➤ 目前盘片颤振抑制研究

By enhancing the disk stiffness



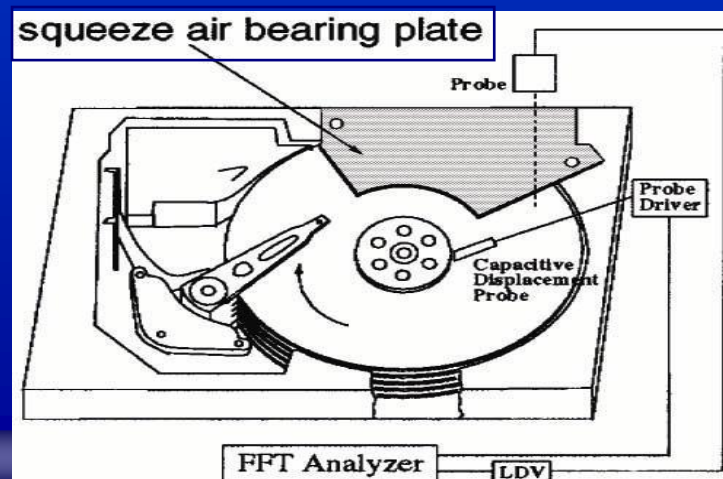
$$\text{Flutter speed} \propto \frac{Eh^2}{12(1-\nu^2)\rho_d r_o^4}$$

By designing the base casting
Heo et al. (2000) [实验]



Reduce disk-rim to shroud gap
Smooth the shroud

By employing air squeeze film
*Bittner and Shen (1999),
Ono and Maeda (2000),
Deeyiengyang and Ono (2001).*[实验]





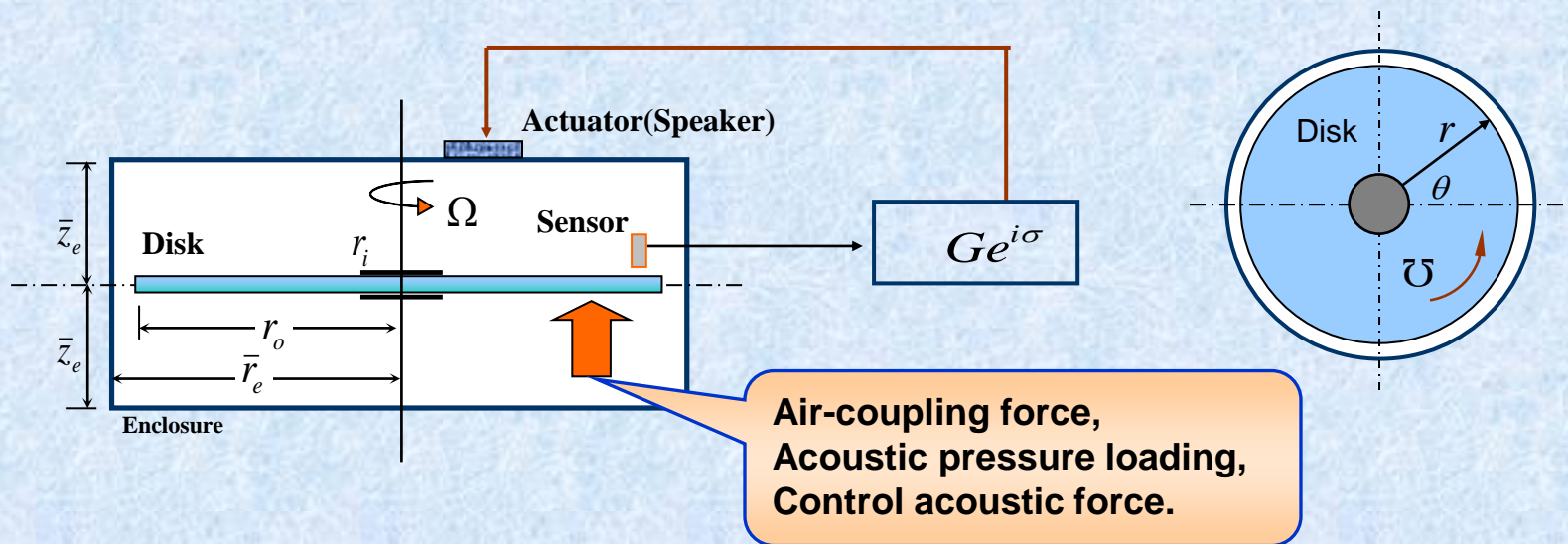
➤ 本文研究

- ✓ 磁盘颤振稳定性分析、临界转速的预测；
- ✓ 提出一种主动控制方式，抑制磁盘颤振失稳；
- ✓ 进行相关实验并给出实验结果；
- ✓ 与理论预测和数值模拟结果进行对比。



❖ THEORETICAL MODELING (理论模型)

• 问题描述



Feature:

- Indirect, non-contact method —— 非接触控制
- 封闭或周边开口



Mathematical Modeling – 数学模型

旋转磁盘振动

Description of rotating disk vibration

$$\frac{\partial^2 w}{\partial t^2} + 2 \frac{\partial^2 w}{\partial t \partial \theta} + \frac{\partial^2 w}{\partial \theta^2} + \mu \nabla^4 w - \left[\frac{1}{r} \frac{\partial}{\partial r} (r \sigma_r \frac{\partial w}{\partial r}) + \frac{1}{r^2} \frac{\partial}{\partial \theta} (\sigma_\theta \frac{\partial w}{\partial \theta}) \right] = q(r, \theta, t)$$

Boundary Condition

a) At the clamped edge:

$$w|_{r=\kappa} = \frac{\partial w}{\partial r}|_{r=\kappa} = 0$$

b) At the free edge:

$$\left[\frac{\partial^2 w}{\partial r^2} + \nu \left(\frac{1}{r} \frac{\partial w}{\partial r} + \frac{1}{r^2} \frac{\partial^2 w}{\partial \theta^2} \right) \right]_{r=1} = 0, \left[\frac{\partial}{\partial r} (\nabla^2 w) + \frac{(1-\nu)}{r^2} \frac{\partial^2}{\partial \theta^2} \left(\frac{\partial w}{\partial r} - \frac{w}{r} \right) \right]_{r=1} = 0$$

空气压力
粘性旋转流体压力
控制力...



Description of loadings of system

(1). Aerodynamic Force Induced By Rotating Disk-Airflow Coupling

-----Rotating Damping Model

$$q_f(r, \theta, t) = -C \left[\frac{\partial w}{\partial t} + \left(1 - \frac{\Omega_d}{\Omega}\right) \frac{\partial w}{\partial \theta} \right]$$

C: Damping coefficient

Ω_d / Ω : Rotation speed ratio

(2). Acoustic Force Induced By Acoustic-Structure Coupling

$$q_a(r, \theta, t) = \Lambda \left[\frac{\partial \phi_a(r, \theta, z = 0^+, t)}{\partial t} - \frac{\partial \phi_a(r, \theta, z = 0^-, t)}{\partial t} \right]$$



Where ϕ_a is the acoustic velocity potential, and is governed by

声场

$$\nabla^2 \phi_a = M^2 \frac{\partial^2 \phi_a}{\partial t^2}$$

$$\begin{aligned} \frac{\partial \phi_a}{\partial r} \Big|_{r=r_e} = 0, \quad \frac{\partial \phi_a}{\partial z} \Big|_{z=\pm z_e} = 0, \quad \frac{\partial \phi_a}{\partial r} \Big|_{r=r_e} = 0, \quad \frac{\partial \phi_a}{\partial z} \Big|_{z=\pm z_e} = 0 \\ \frac{\partial \phi_a}{\partial z} \Big|_{z=0} = \begin{cases} 0 & (0 \leq r < \kappa) \\ \frac{\partial w}{\partial t} & (\kappa \leq r \leq 1) \end{cases}, \quad \phi_a \Big|_{z=0} = 0 \quad (1 < r \leq r_e) \end{aligned}$$

The boundary conditions, match conditions on the disk surface and at the clearance between the disk rim and enclosure:



(3). Acoustic Control Force Induced By Actuator

$$q_c(r, \theta, t) = \Lambda \frac{\partial \phi_c(r, \theta, z = 0^+, t)}{\partial t}$$

Where ϕ_c is the acoustic velocity potential, and is governed by

$$\bar{\nabla}^2 \phi_c = M^2 \frac{\partial^2 \phi_c}{\partial t^2}$$

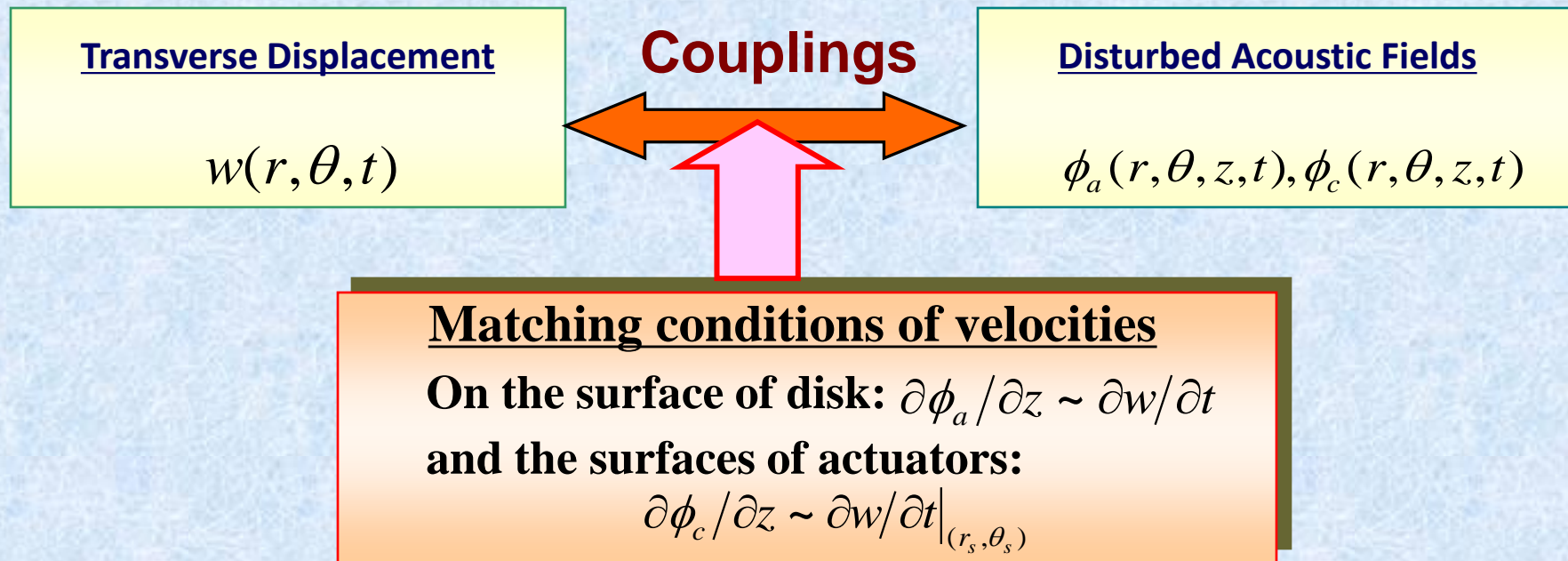
控制声场

$$\left. \frac{\partial \phi_c}{\partial z} \right|_{z=0} = 0, \quad \left. \frac{\partial \phi_c}{\partial r} \right|_{r=r_e} = 0, \quad \left. \frac{\partial \phi_c}{\partial z} \right|_{z=z_e} = \begin{cases} a_n(r) e^{in\theta} \frac{\partial w}{\partial t} \Big|_{(r_s, \theta_s)} & ((r, \theta) \in S_a) \\ 0 & ((r, \theta) \notin S_a) \end{cases}$$



■ Solutions – 半解析半数值求解

○ Characteristics



- Difficulties arising from couplings
- All equations should be solved synchronously



■ Solutions – 半解析半数值求解

假设含有参数的变形场、声场的解

$$w(r, \theta, t) = \sum_{m=0}^{\infty} c_m R_{mn}(r) e^{i(n\theta + \lambda t)}$$

$$\phi_a = \sum_{k=1}^{\infty} d_k^a \cosh[\alpha_k(z_e - z)] J_n(\xi_k r) e^{i(n\theta + \lambda t)},$$

$$\phi_c = \sum_{k=1}^{\infty} d_k^c \cosh(\alpha_k z) J_n(\xi_k r) e^{i(n\theta + \lambda t)}$$

w, ϕ_a, ϕ_c satisfy partial boundary conditions or governing equations

(m,n): Disk vibration mode
m =: Nodal circle number
n =: Nodal diameter number
 λ =: Eigenvalue

Equation of disk vibration



$[\mathbf{c}]$ -- unknown
coefficient matrix

$[\mathbf{B}]$ -- free vibration of
rotating disk

$[\mathbf{P}^f], [\mathbf{P}^a], [\mathbf{P}^c]$

-- aerodynamic, acoustic,
control forces

Galerkin's Method

$$\{[\mathbf{B}] + [\mathbf{P}^f] + [\mathbf{P}^a] + [\mathbf{P}^c]\}[\mathbf{c}] = [\mathbf{0}]$$

Nontrivial Solution

$$\det\{[\mathbf{B}] + [\mathbf{P}^f] + [\mathbf{P}^a] + [\mathbf{P}^c]\} = 0$$

Natural Frequency
 $\text{Re}(\lambda)$

Eigenvalues λ
($\lambda^{\text{FTW}}, \lambda^{\text{BTW}}$)

'Damping'
 $\text{Im}(\lambda)$

> 0

Stable

< 0

Unstable
(Flutter)



■ Simulation results

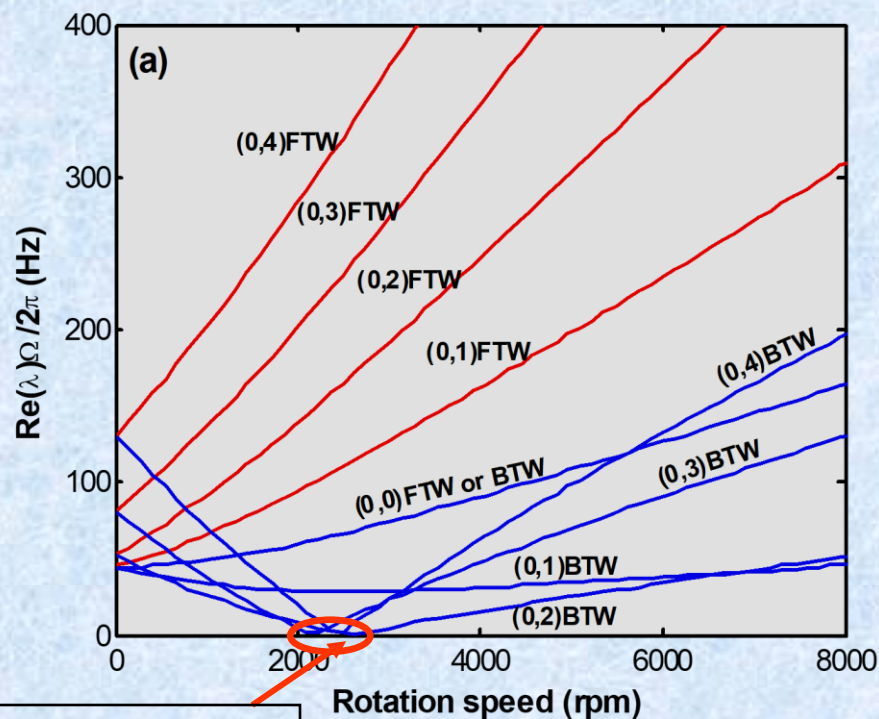
➤ Material & geometric properties

Disk	Density, ρ_d (Kg/m ³)	7.8X10 ³
	Outer radius, r_o (m)	0.178
	Clamping ratio, κ	0.3
	Thickness, h (m)	0.775
	Young's modulus, E (GPa)	200
	Possion's ratio, ν	0.3
Enclosure	Radius, r_e/r_o	1.2
	Height, z_e/r_o	0.5
Airflow	Density, ρ_a (Kg/m ³)	1.21
	Speed of sound, a (m/s)	340

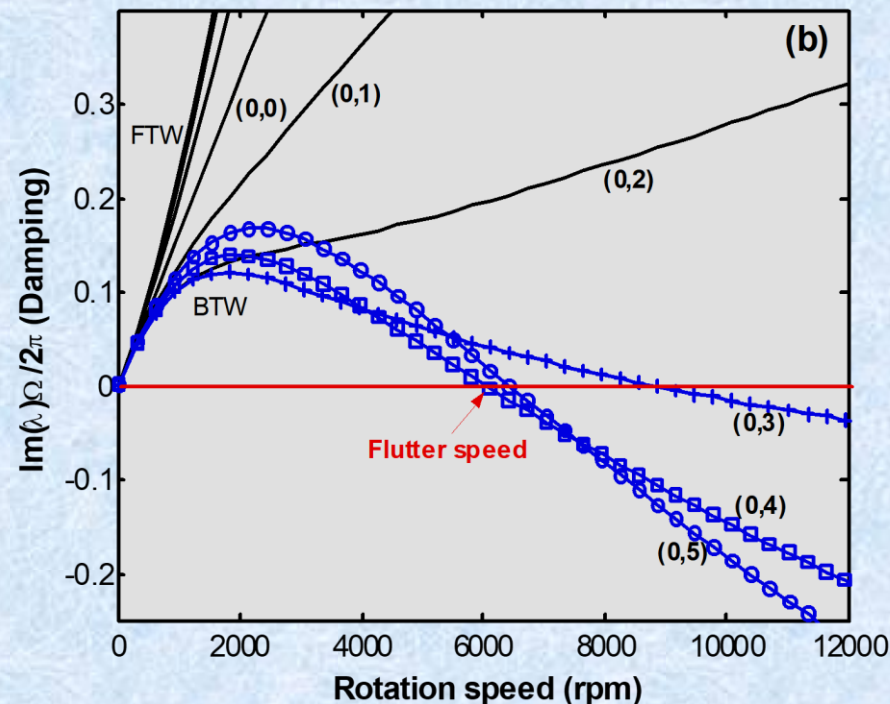
★ The properties of disk same as the ones used in D'Angelo et al's experiment.



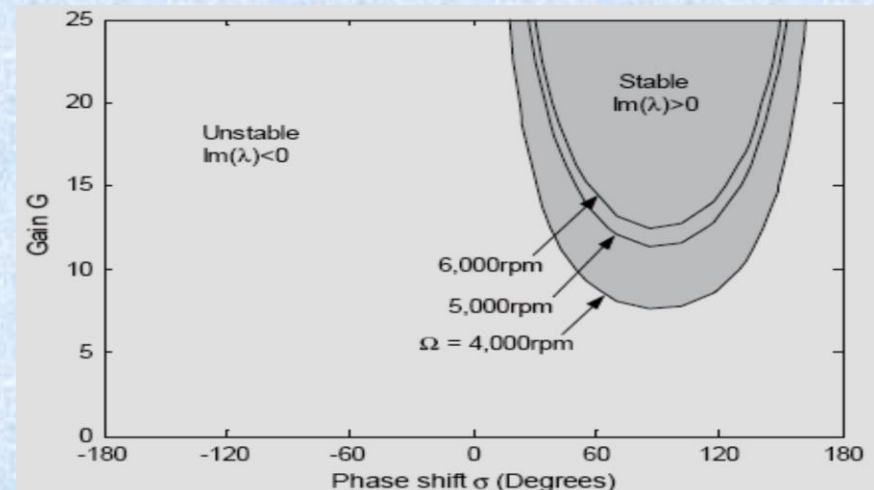
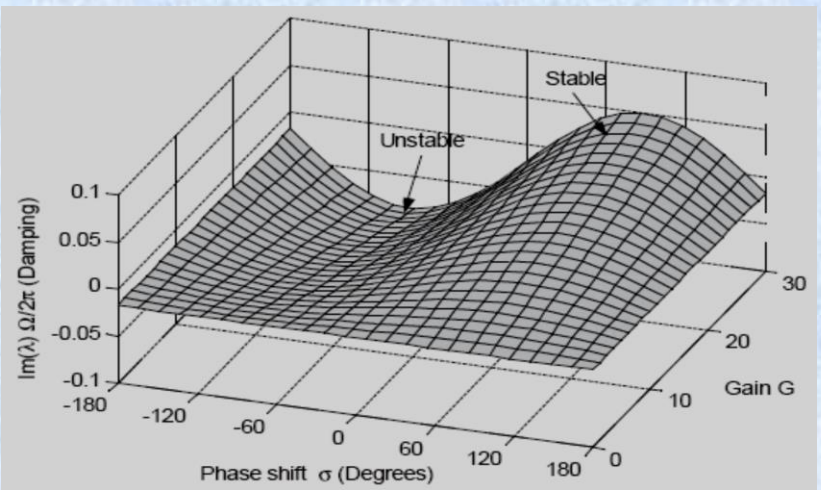
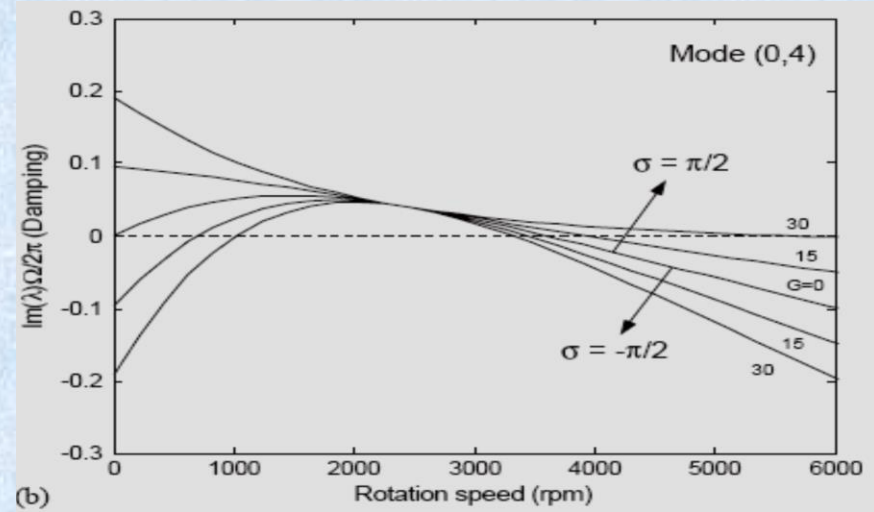
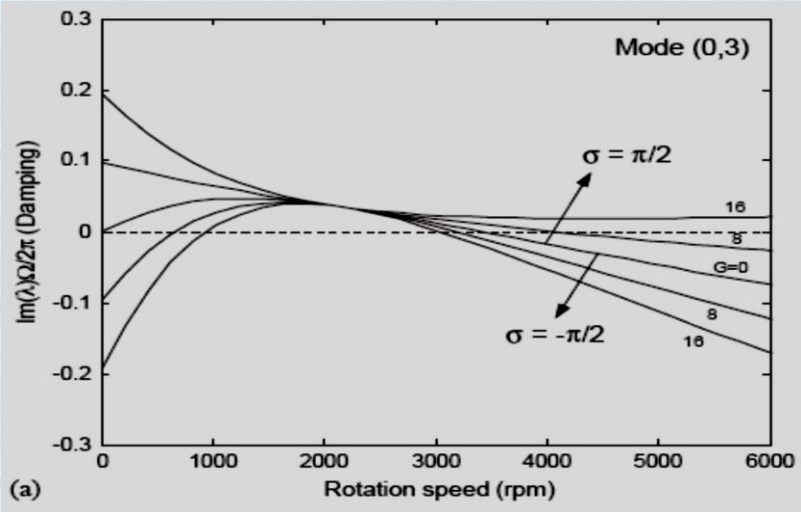
➤ Verifications & Observations of Disk Flutter ($C=0.02; \Omega_d/\Omega=2/3$)



Critical speed



(a) Real part of eigenvalue or mode frequency (b) Imaginary part of eigenvalue or damping

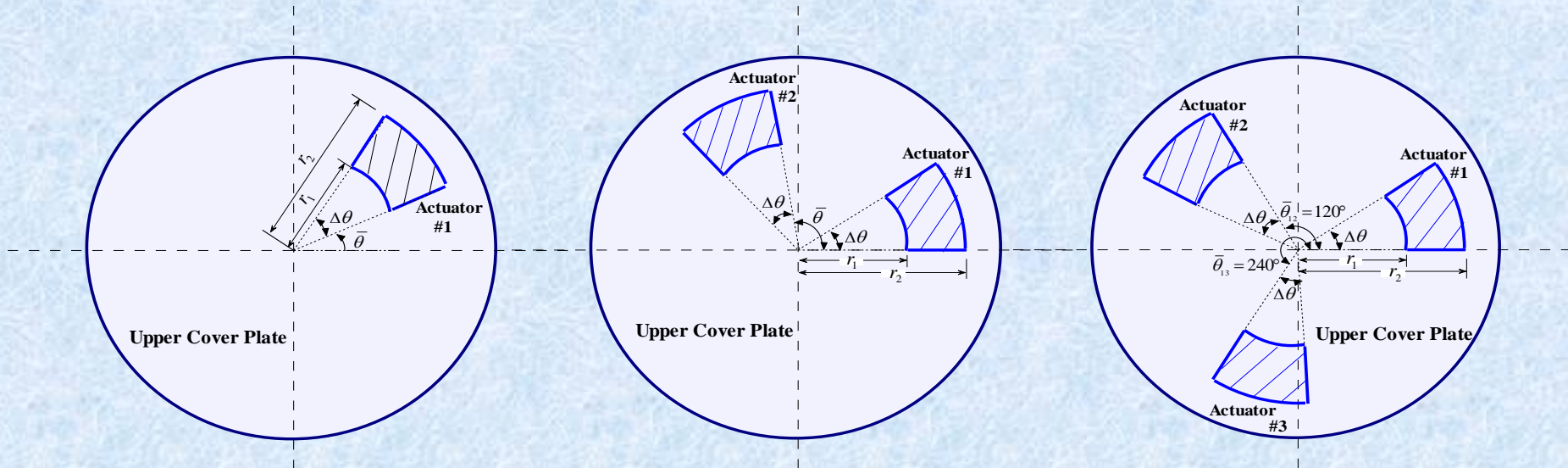


- ✓ The feedback control method proposed can suppress disk flutter effectively
- ✓ The actuating system has a large operation region and therefore it is robust

Huang, X, Wang X, J. Fluid & Structures, 2004



➤ Control Performance & Optimization



Case (a). One Piezo-patch

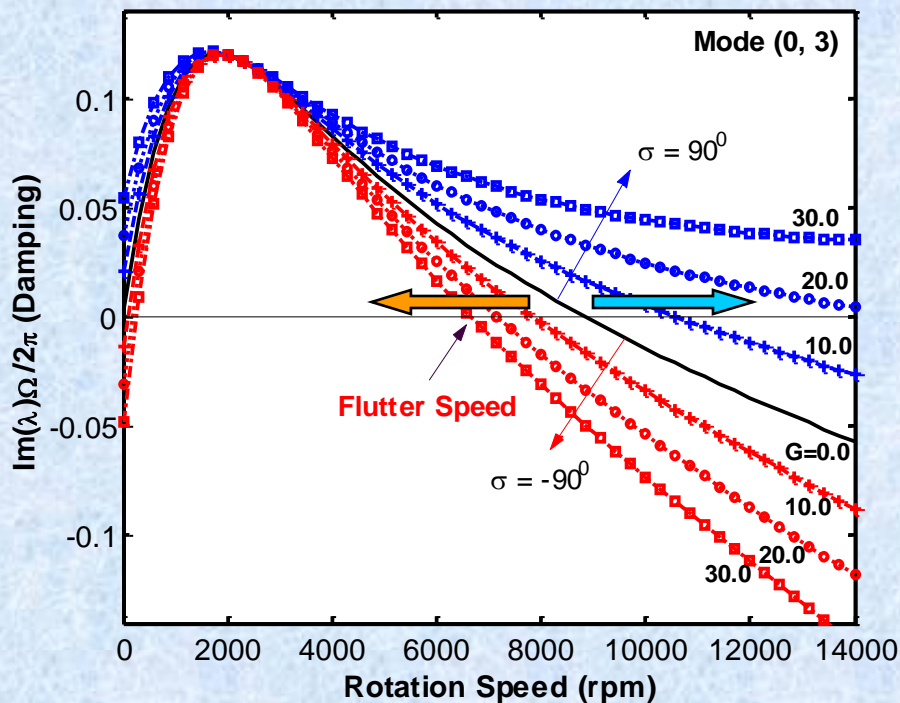
Case (b). Two Piezo-patches

Case (c). Three Piezo-patches

Schematic diagram of Piezo-patch(es) arrangement on the upper cover plate surface

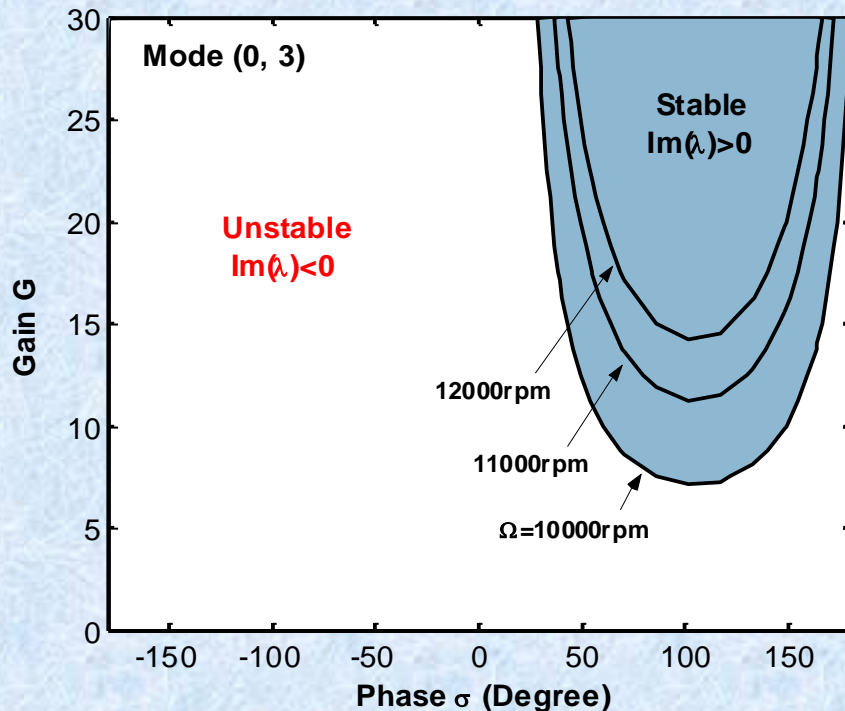


► *Case (a) -- One piezo-patch actuator*



(a) Damping vs. Rotation speed

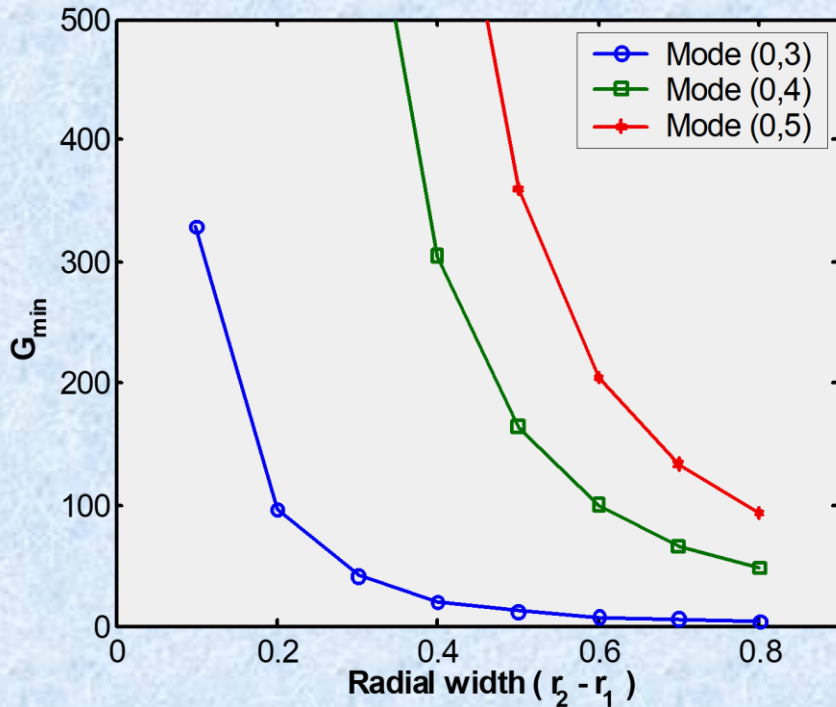
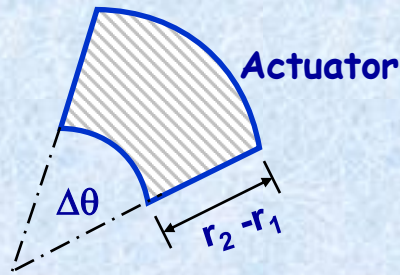
(b) Stability Map in G - σ plane



Control performance for one actuator with $r_1=0.7, r_2=1.0$, and $\Delta\theta=10^\circ$

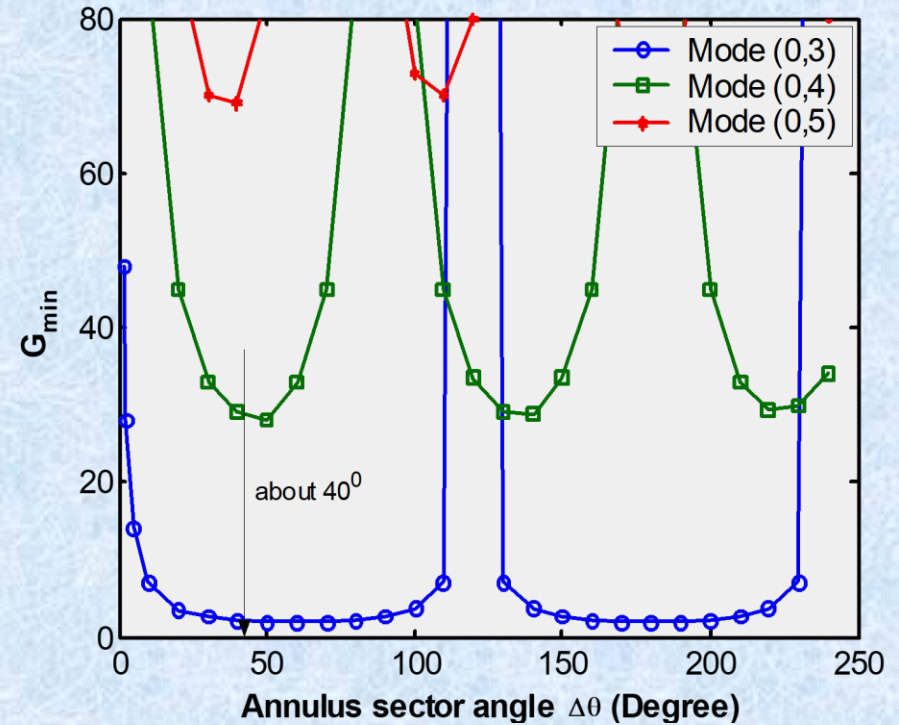


Case (a)



(a) G_{min} vs. Radial width (Fixed $\Delta\theta=10^\circ$)

(b) G_{min} vs. Sector angle $\Delta\theta$ (Fixed $r_1=0.7, r_2=1.0$)



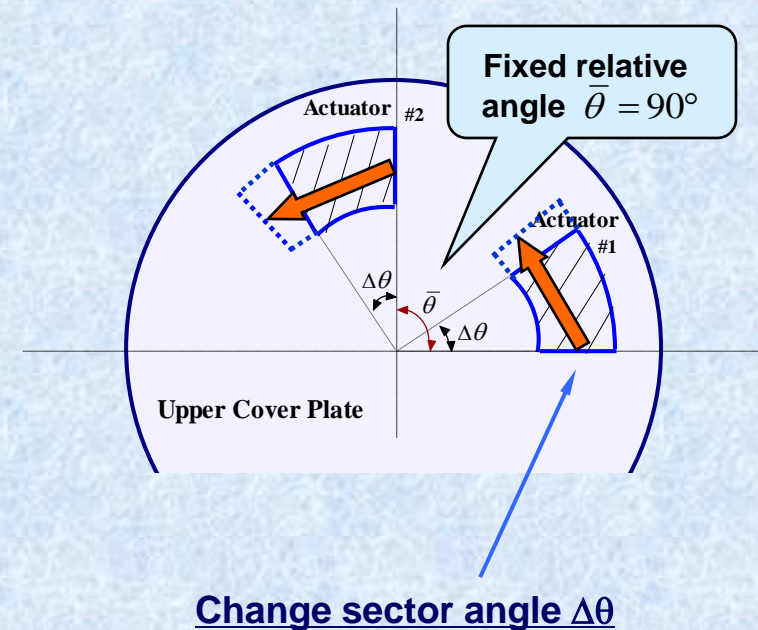
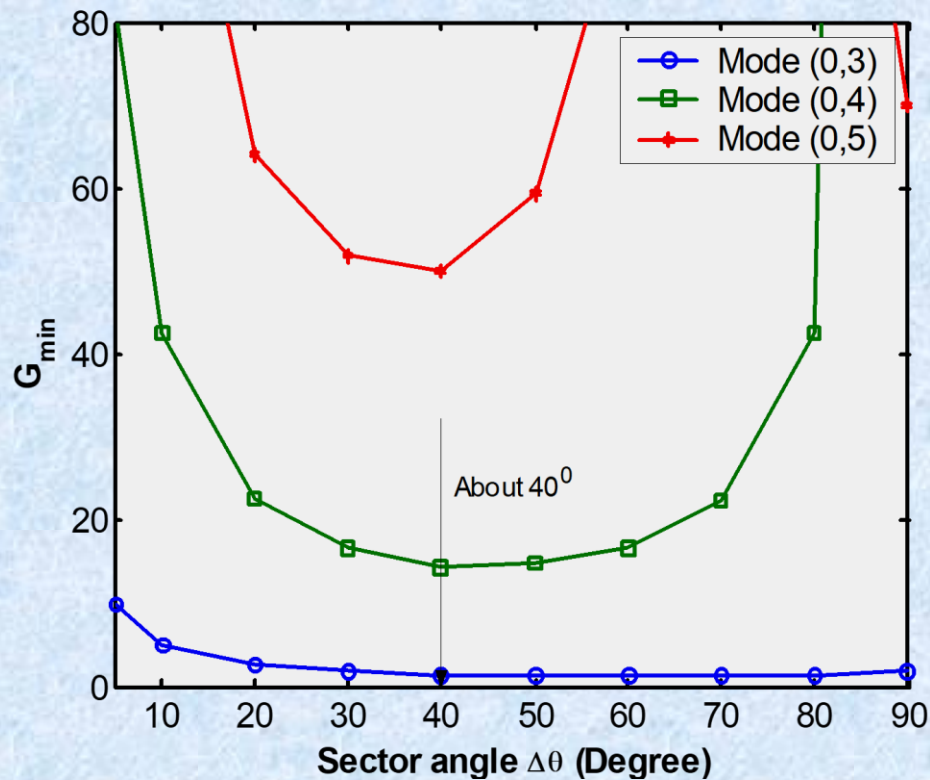
- ❖ **Disable for control:**
 - $\Delta\theta=120^\circ$ for mode (0,3);
 - $\Delta\theta=90^\circ, 180^\circ$ for mode (0,4);
 - $\Delta\theta=72^\circ, 144^\circ, 216^\circ$ for mode (0,5).

Effect of actuator size on control performance for one actuator



► *Case (b) -- Two piezo-patches ($G_1 = G_2, \sigma_1 = \sigma_2$)*

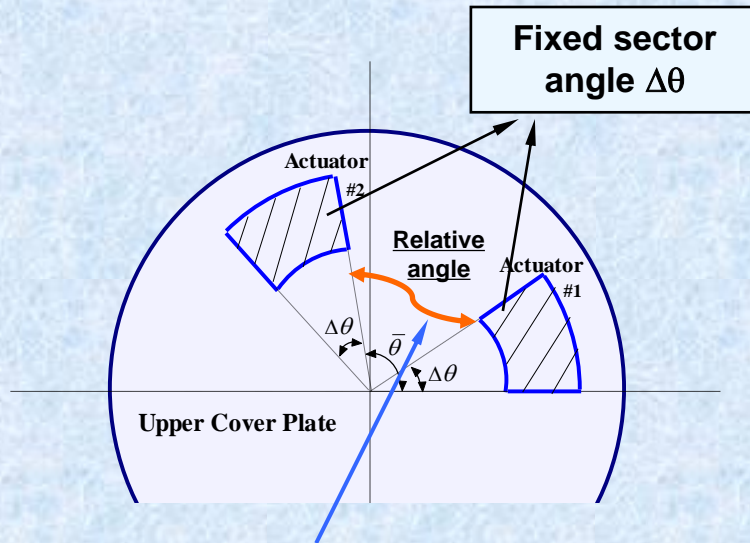
(a) G_{\min} vs. Sector angle $\Delta\theta$ (Fixed $\bar{\theta} = 90^\circ$)



Control performance for two actuators



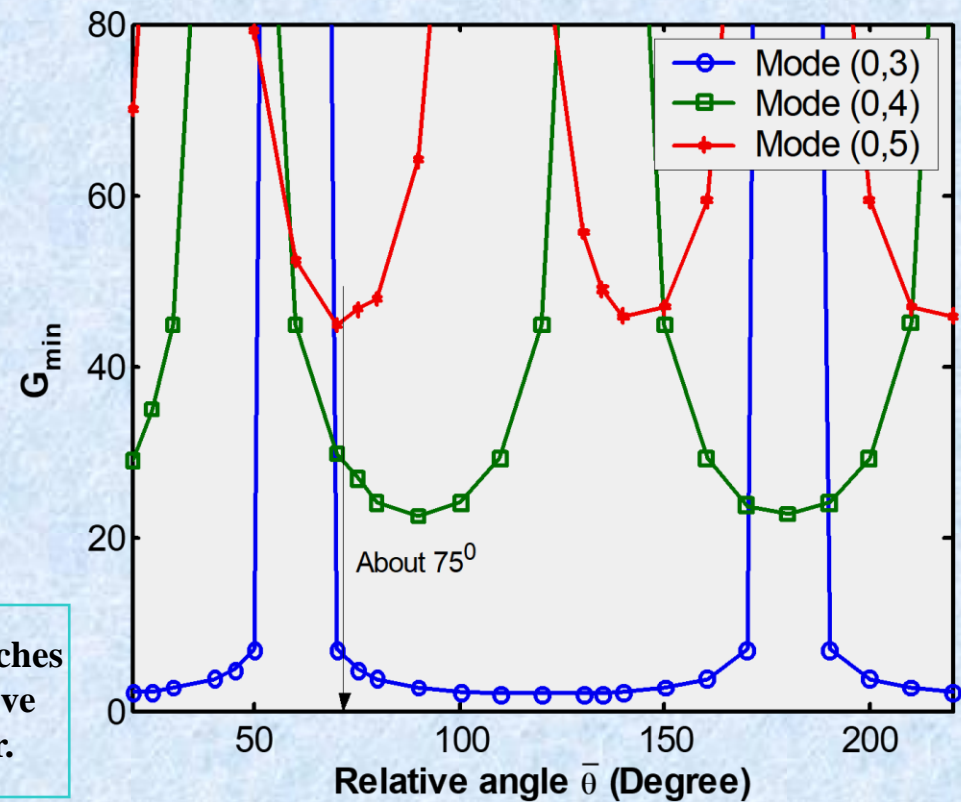
Case (b)



Change relative angle

❖ By dividing one patch into two patches and arranging with a proper relative angle, the control gains are smaller.

(b) G_{min} vs. Relative angle $\bar{\theta}$ ($\Delta\theta=40^\circ/2$)

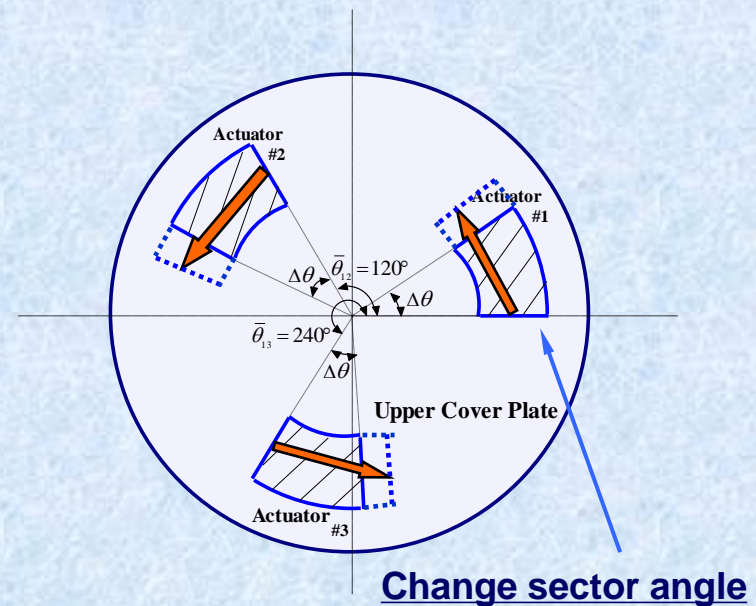
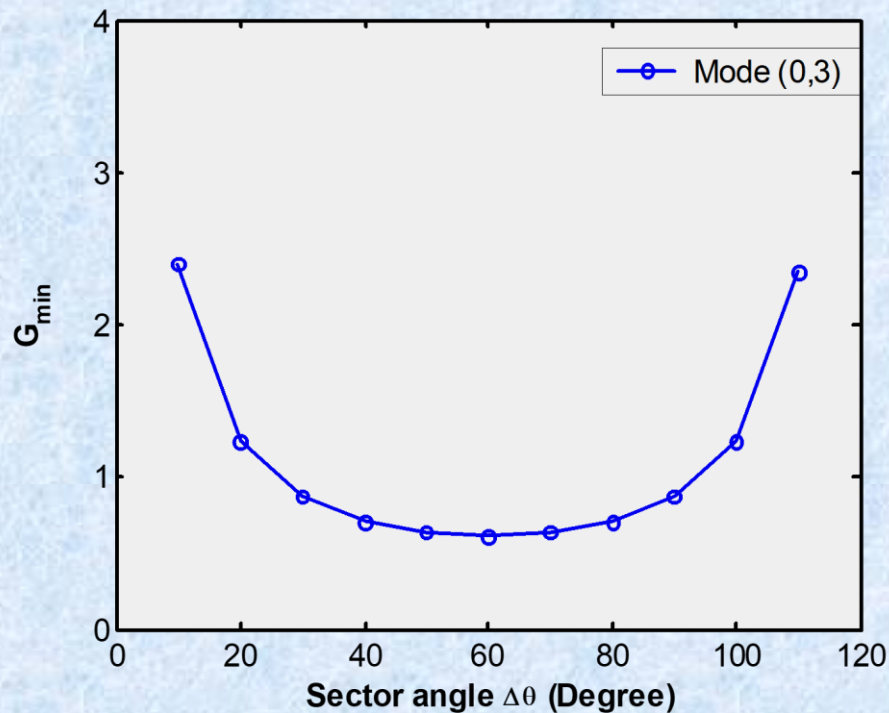


Control performance for two actuators



■ *Case (c) -- Three piezo-patches* ($G_1 = G_2 = G_3$)

(a) G_{min} vs. Sector angle $\Delta\theta$ ($\sigma_1 = \sigma_2 = \sigma_3$)



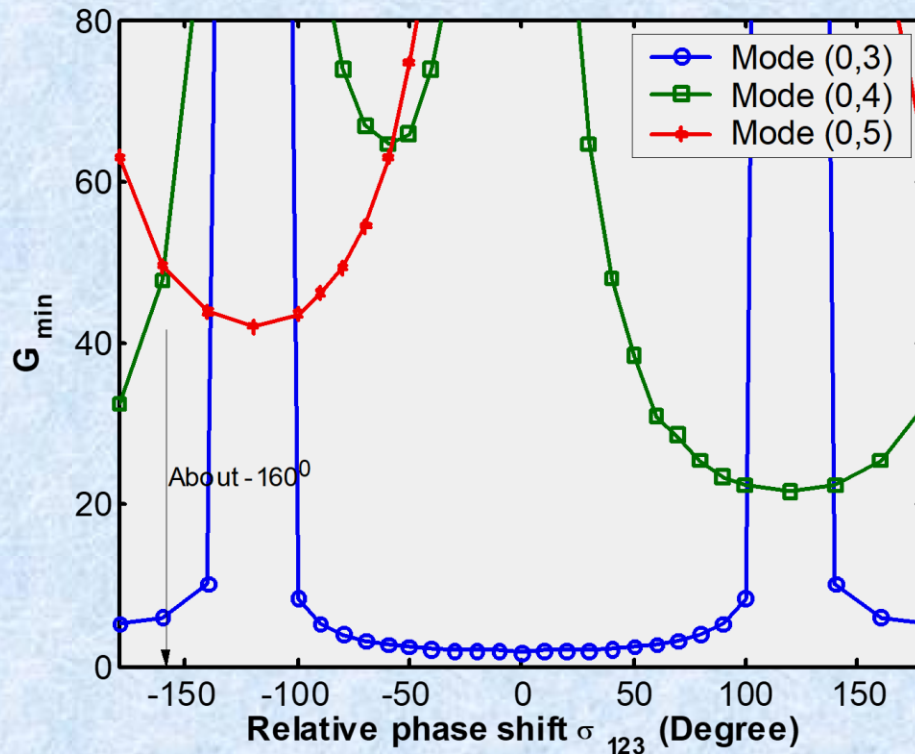
❖ Flutter control for modes (0,4) and (0,5) is disable.

Control performance for three actuators



Case (c)

(b) G_{\min} vs. Relative phase shift σ_{123}



- Fixed locations.
- Fixed size $\Delta\theta=40^\circ/3$.
- Different phase shift:
 $\sigma_1, \sigma_2=\sigma_1+\sigma_{123}, \sigma_3=\sigma_2+\sigma_{123}$.

Control performance for three actuators

Wang X, Huang, X, AIAA Journal, 2006



程序设计相关问题

1. 程序设计的一般原则



❖ 针对具体问题的特点选择合适的数值方法

- 问题的复杂程度，数学描述的可选途径 —— 理论知识
- 各种方法的优缺点要有认识 —— 阅读与学习
- 多种方法的联合使用 —— 比较与思考
- 可优先考虑自己所熟悉掌握的方法 —— 自身优势、事半功倍

❖ 使用商业软件或二次开发、或完全编写代码

- 直接使用——了解商业软件的功能，特别是耦合场分析能力
- 二次开发——商业软件的开放性、可开发性
- 编写代码——各个物理或者力学场分析方法的实现、零散代码的利用与集成



❖ 相关数值算法的掌握

- 基本的：矩阵运算、微积分运算、排序、特殊函数等
- 特别的：
 - ✓ 迭代算法（收敛性、稳定性）
 - ✓ 特征值问题（线性、非线性）
 - ✓ 动力学问题（Wilson- θ 、Newmark方法等）
 - ✓ 非线性方程算法（Newton法、Newton-Raphson法、最速下降法、共轭梯度法等）
 - ✓ 图形图像处理等



❖ 程序设计思想

- 分场、依次对涉及的多场问题进行程序设计，确定输入量、输出量
- 采用合适的算法处理场-场耦合，迭代算法的收敛条件等
- 联系各个场之间的数据传输与处理
- 最终输出结果的表征（图像图像等）



❖ 程序调试与结果的可靠性判断

- 最耗时、长期的、也是计算能力的体现
- 合适的考题验证数值编码的正确性
 - ✓ **局部验证**——每一个子程序、每一个场的验证：解析解、退化结果、对称性、不同的软件、算法求解统一问题比较等、结果稳定性的验证（不同的单元剖分、节点数目的变化、边界条件的变化、空间和时间步长的变化等）
 - ✓ **全局验证**——各个场串起来的验证：特例（单向、解耦情形）、各场之间联系环节的验证、整体收敛性、稳定性的验证（迭代终止条件的选择、优化参数选取）、结果的初步判定（定性上是否正确？有无力学、物理的合理解释？稳定性？）

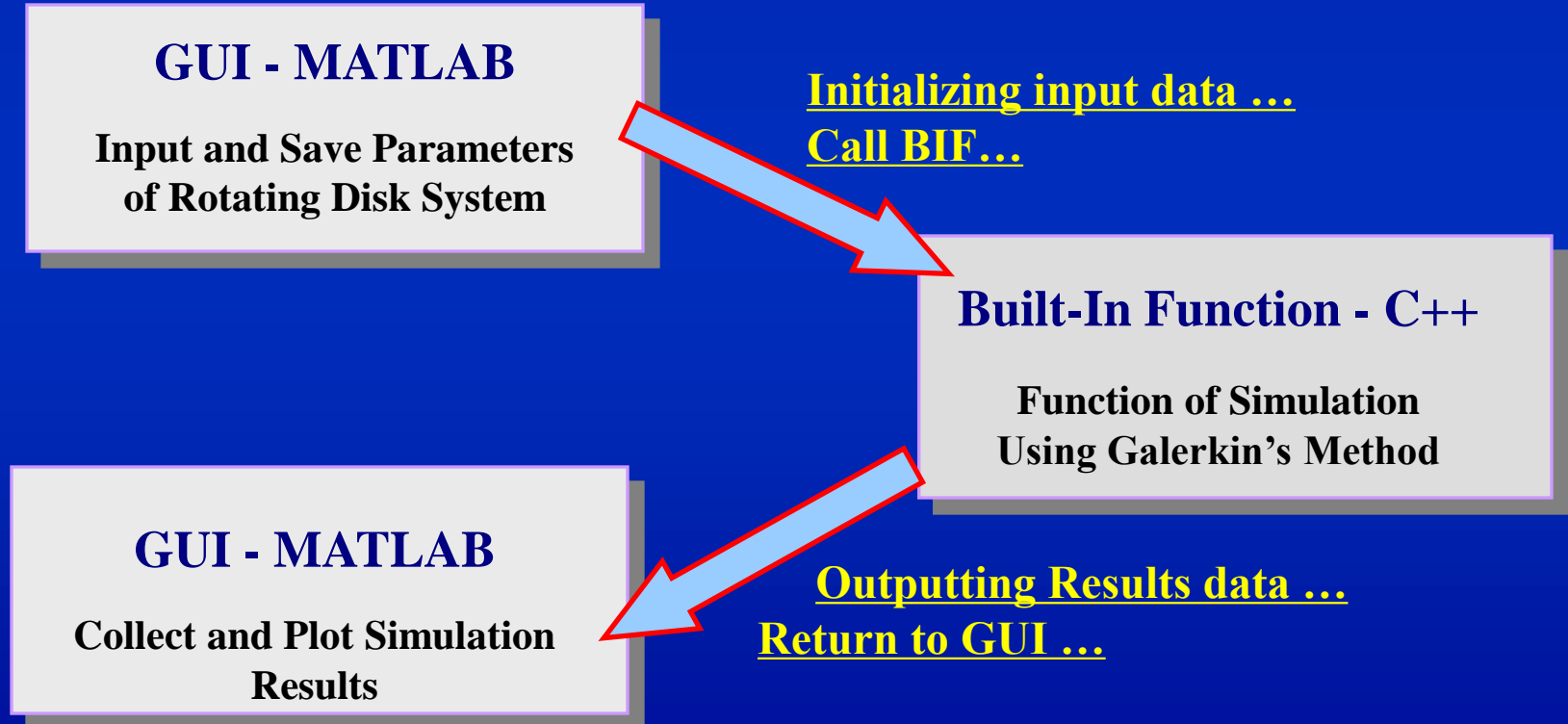


程序设计相关问题

2. 旋转圆盘振动与控制软件包介绍

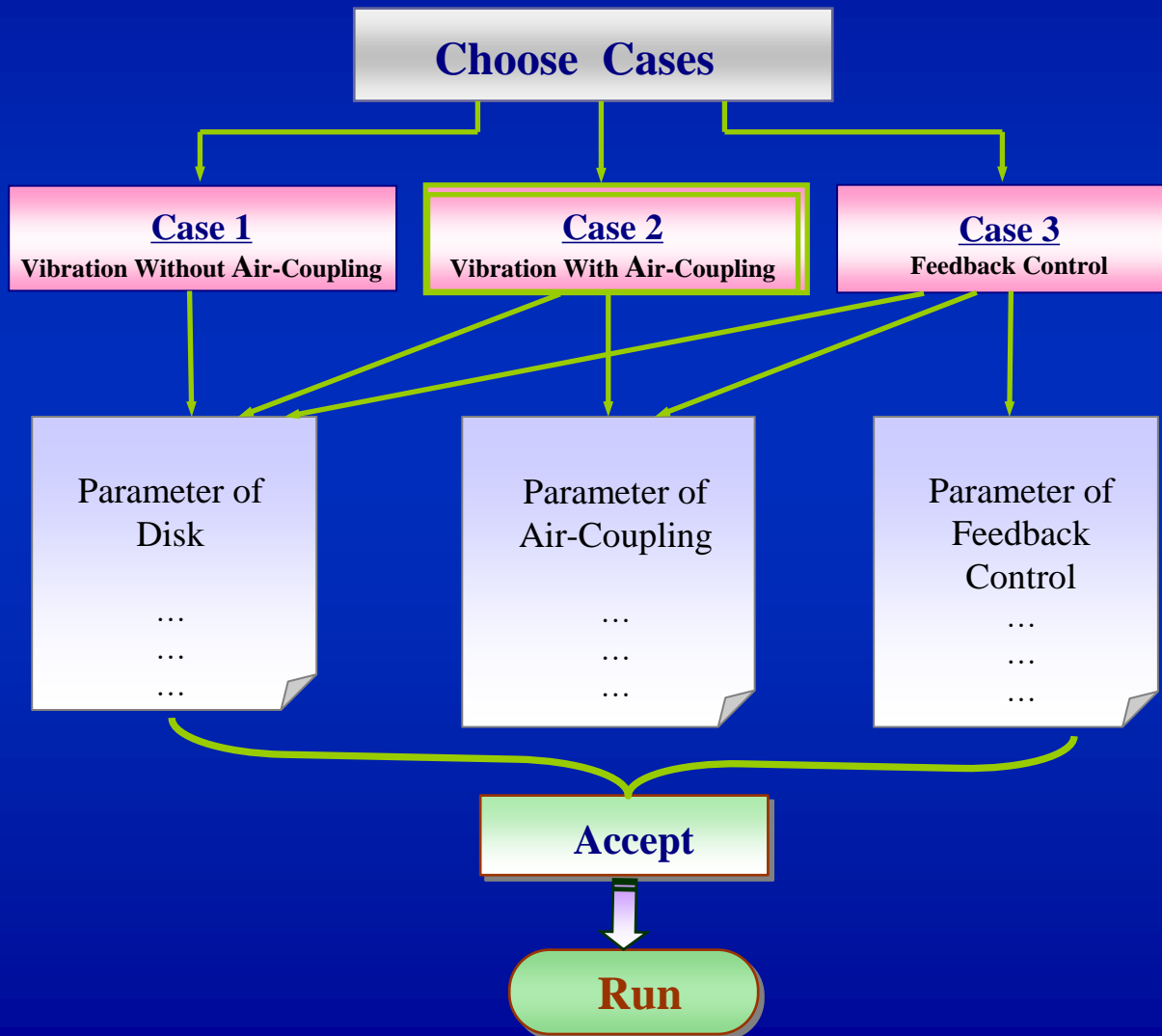


Implementation Flowchart

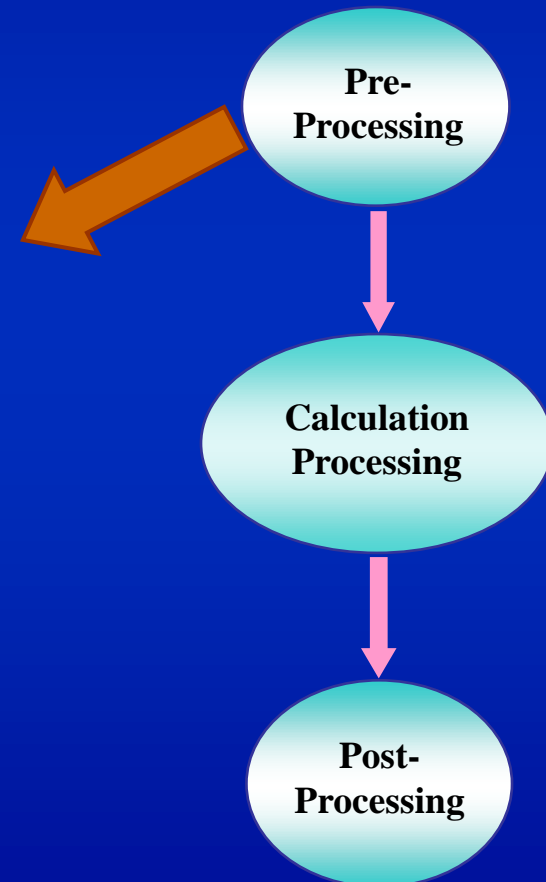




Pre-Processing

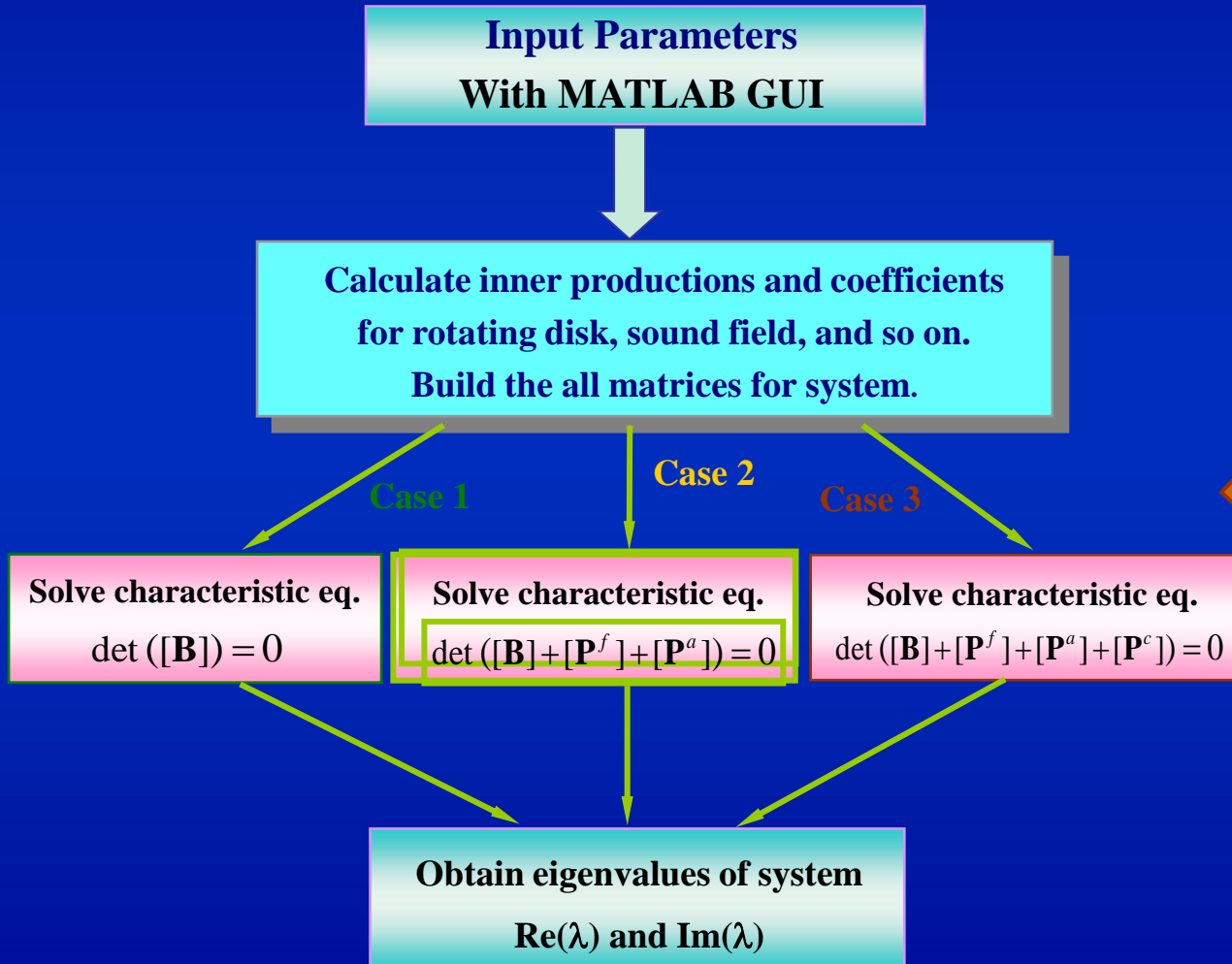


Flowchart





Calculation Processing



Flowchart

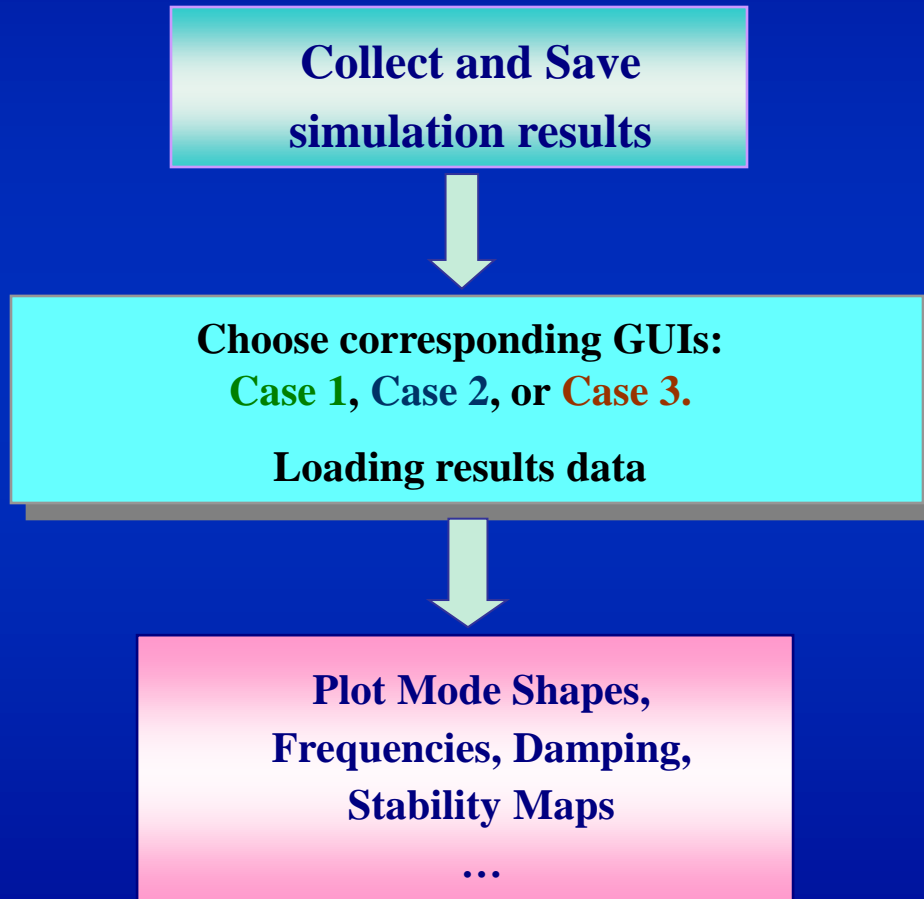
Pre-
Processing

Calculation
Processing

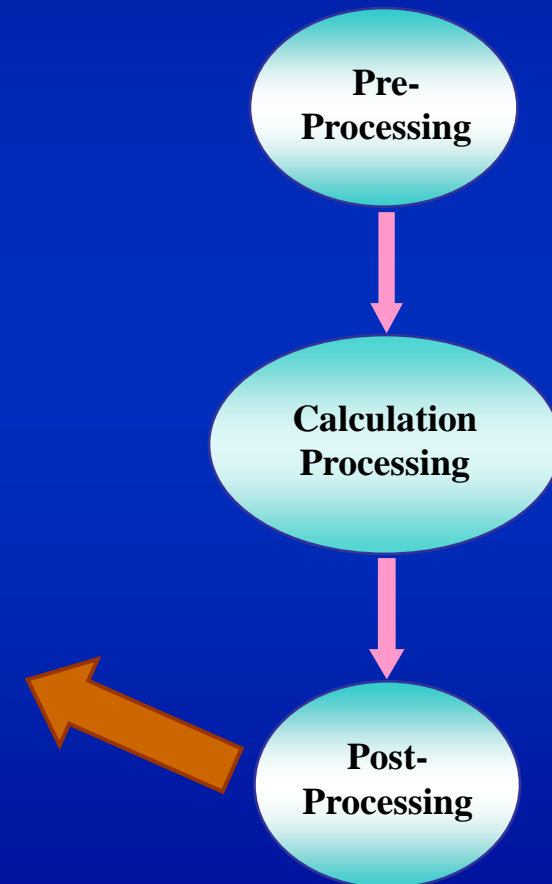
Post-
Processing



Post-Processing



Flowchart





Main User Interactive Menu

Pulldown
Menu

RotatingDiskVibration
File Run Results Help

Aeroelastic Vibration and Feedback Control of Rotating Disk

Parameter of Disk

Outer Radius: Input R_o (m)

Inner Radius: Input R_i (m)

Thickness: Input h (m)

Density: Input (kg/m^3)

Young's Modulus: Input E (Pa)

Possion's Ratio: Input value

Rotation Speed (Rpm)

From Initial value To Ending value

Function (Only one Chosen)

Vibration Without Air-Coupling

Vibration With Air-Coupling

Feedback Control

Parameter of Air-Coupling

Air-Loading Coefficient: 0.005
0.01
0.02

Rotation Ratio: 0.67
0.70
0.75

Enclosure Size:

Radius 1.1 R_o Height 0.1 R_o

Parameter of Feedback Control

Location of Sensor:

R_s 0.7 R_o Theta 0 (Degree)

Actuator Radius: 0.4 R_o

Gain of Controller

From Initial value To Ending value

Phase Shift of Controller (Degree)

From Initial value To Ending value

Accept Run Reset



User Interactive Menu – Result Plot 1

RESULTS: Mode Shape

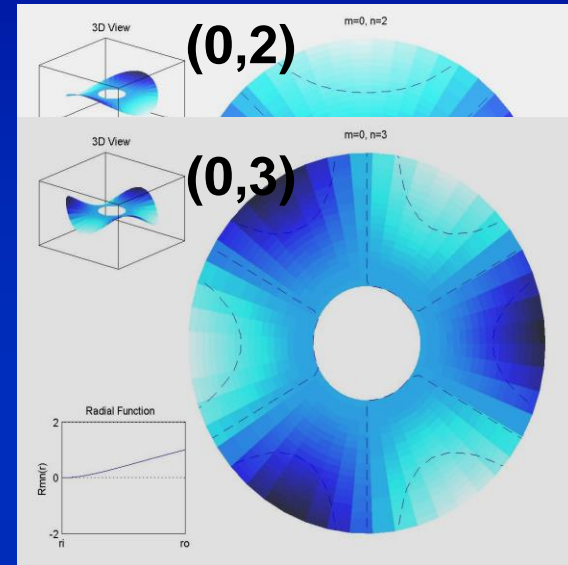
File Edit View Insert Tools Window Help

Vibration Mode: Nodal circle $m = 0$ Nodal diameter $n = 4$

3D View

Operation

- Load Data
- 3D View
- 2D View
- Animation
- Radial Shape
- Clear



Animation

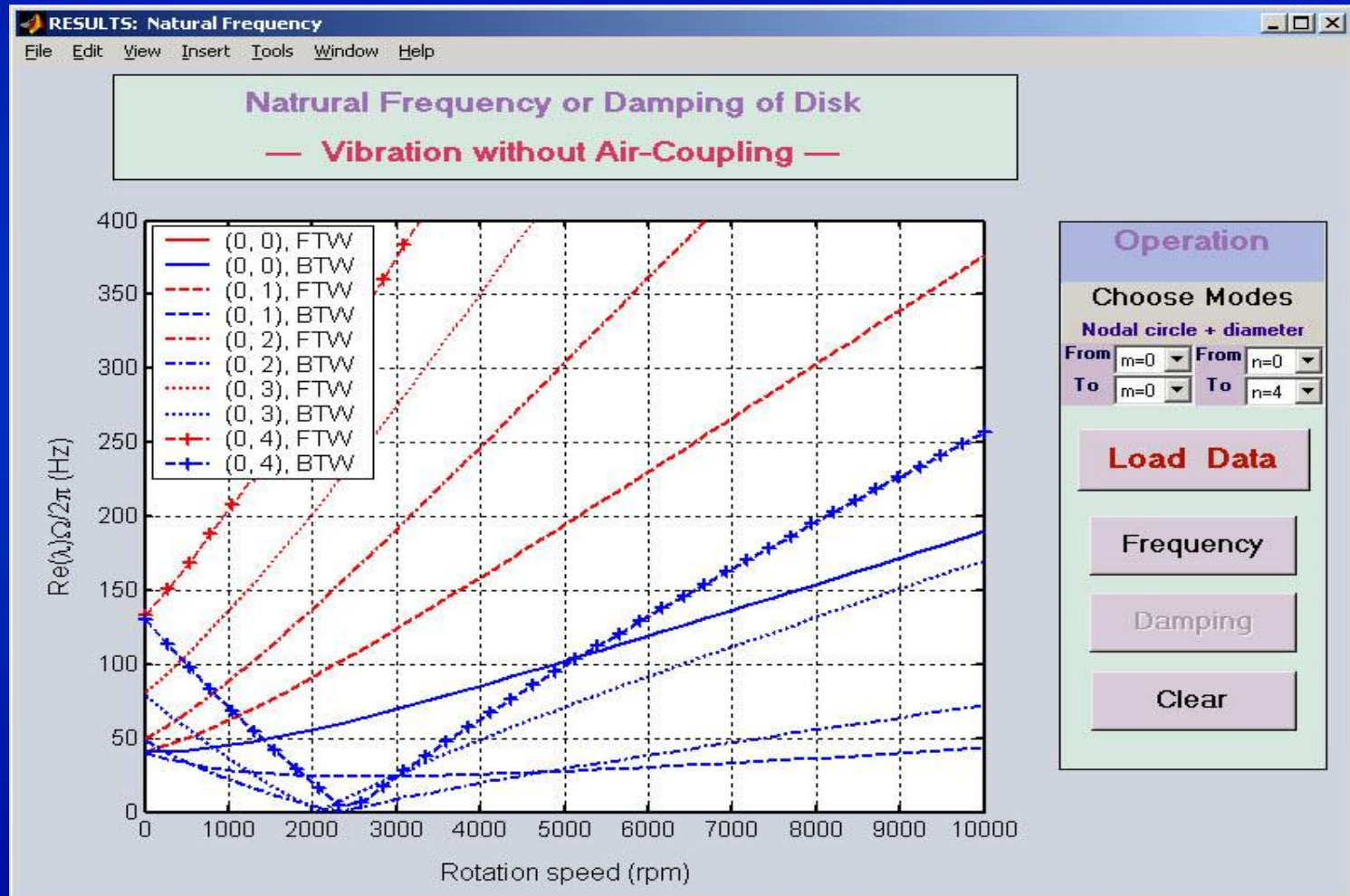
Select a operation for animation:

- Free Vibration - Rotation System (or no-rotating disk)
- Free Vibration - Fixed System - FTW
- Free Vibration - Fixed System - BTW
- Free Vibration - Fixed System - FTW & BTW
- Unstable Vibration - Rotation System
- Unstable Vibration - Fixed System - FTW
- Unstable Vibration - Fixed System - BTW
- Unstable Vibration - Fixed System - FTW & BTW
- Controlled Vibration - Rotation System
- Controlled Vibration - Fixed System - FTW
- Controlled Vibration - Fixed System - BTW
- Controlled Vibration - Fixed System - FTW & BTW

Ok Cancel

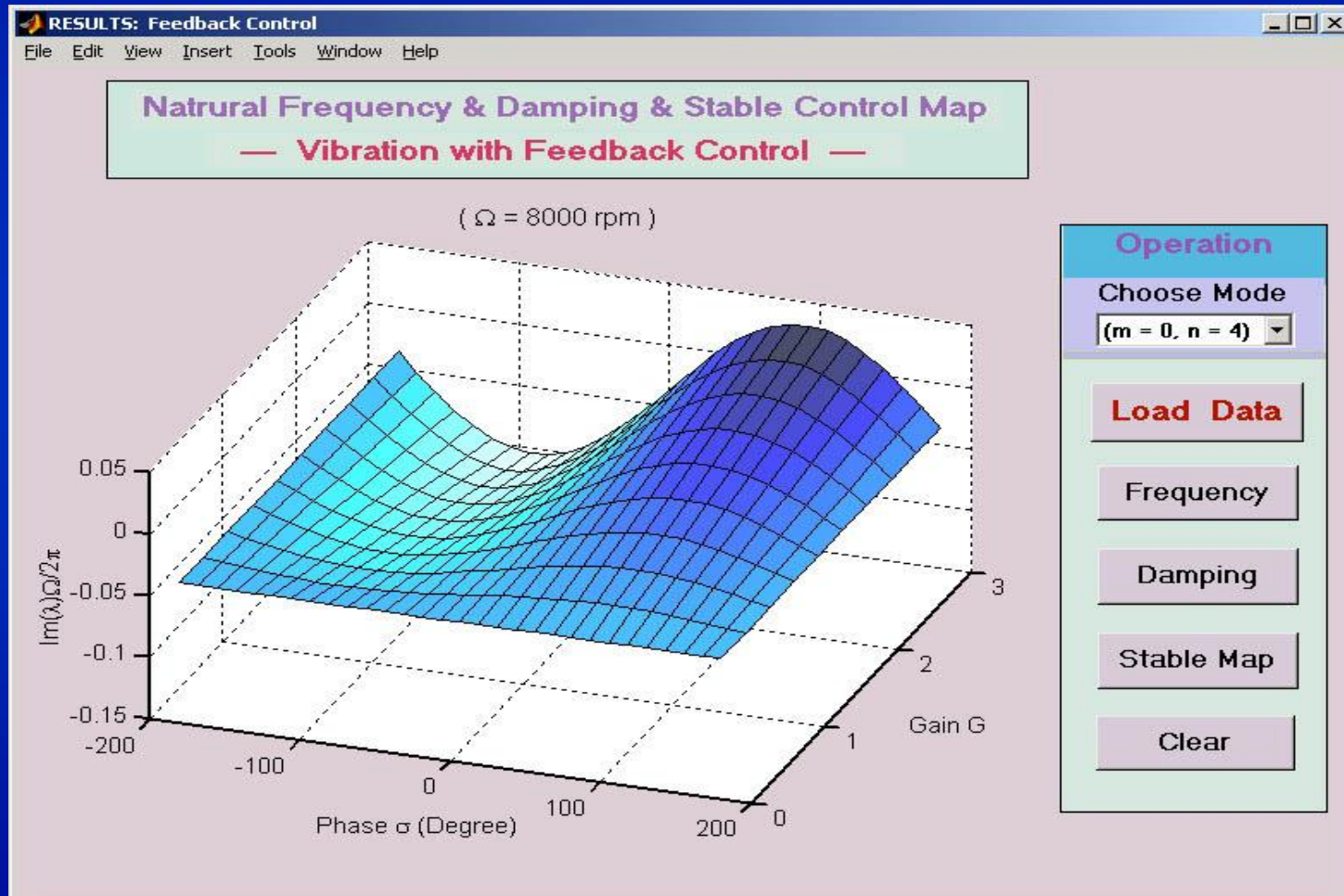


User Interactive Menu – Result Plot 2





User Interactive Menu – Result Plot 3



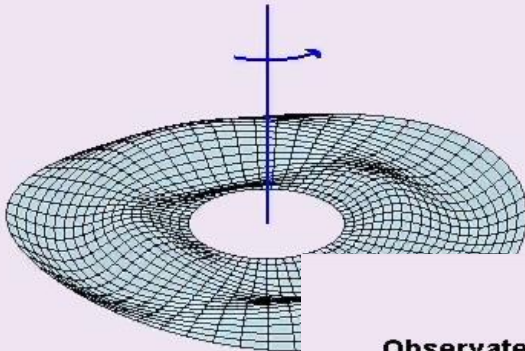


Appendix.

Forward Traveling Wave

STOP

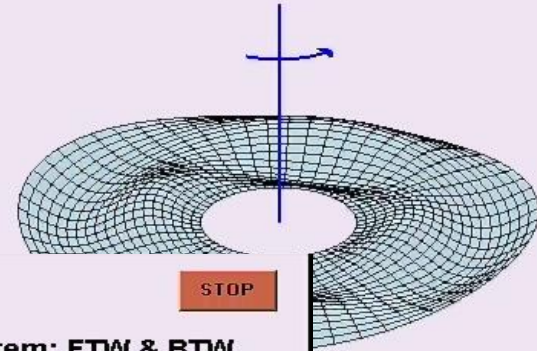
Observed in Fixed Coordinate System: FTW



Backward Traveling Wave

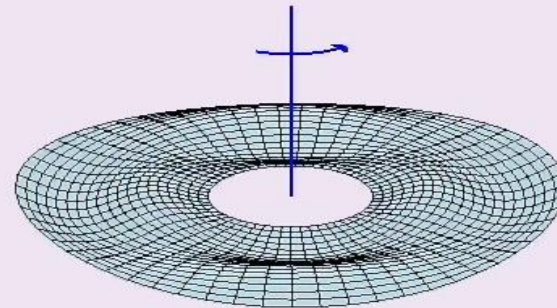
STOP

Observed in Fixed Coordinate System: BTW



STOP

Observed in Fixed Coordinate System: FTW & BTW





Thanks !